MATHEMATICAL ENGINEERING
TECHNICAL REPORTS

Stable Economic Agglomeration Patterns in Two Dimensions: Beyond the Scope of Central Place Theory

Kiyohiro IKEDA, Kazuo MUROTA,
and Yuki TAKAYAMA

METR 2014–24 September 2014

DEPARTMENT OF MATHEMATICAL INFORMATICS
GRADUATE SCHOOL OF INFORMATION SCIENCE AND TECHNOLOGY
THE UNIVERSITY OF TOKYO
BUNKYO-KU, TOKYO 113-8656, JAPAN

WWW page: http://www.keisu.t-u-tokyo.ac.jp/research/techrep/index.html

Stable economic agglomeration patterns in two dimensions: beyond the scope of central place theory[1]

Kiyohiro Ikeda,[2] Kazuo Murota,[3] Yuki Takayama[4]

Abstract

This paper elucidates which agglomeration patterns are stable in two-dimensional uniform economic space and how such patterns appear under decreasing transport costs. Hexagonal lattices with and without boundary are advanced respectively as suitable theoretical and practical spatial platforms of economic activities. Agglomeration patterns on these lattices contain hexagons in central place theory, but also encompass megalopolis and racetrack-shaped de-centralization, which are beyond the scope of central place theory. When the transport cost decreases, stable economic agglomeration undergoes the formation of the smallest hexagon and gradual transition to patterns with larger market areas, often undergoing downtown decay but finally leading to a megalopolis.

JEL: R12, R13, C65, F12

Keywords: bifurcation; central place theory; hexagonal lattice; spatial agglomeration; stability; transport cost

[1]Support of Scientific Research (B) 19360227/21360240/ 24360202 from JSPS is appreciated.

[2]Address for correspondence: Kiyohiro Ikeda, Department of Civil Engineering, Tohoku University, 6-6-06 Aoba, Sendai 980-8579, Japan; ikeda@civil.tohoku.ac.jp.

[3]Department of Mathematical Informatics, University of Tokyo, Tokyo 113-8656, Japan

[4]Department of Civil Engineering, Tohoku University, 6-6-06 Aoba, Sendai 980-8579, Japan

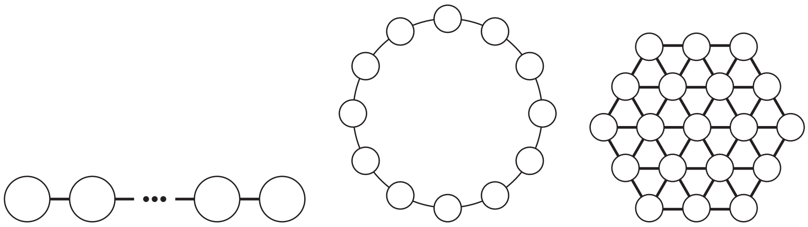

Figure 1: Spatial platforms for economic activities. Circles represent places and lines denote roads.

1. Introduction

Economic agglomeration displays various spatial patterns serving as a cradle of development and prosperity. Cities and towns in southern Germany are spread out and led to the finding of hexagonal distributions in central place theory (Christaller, 1933 [6]). In North America, a chain of cities is distributed from Boston to Washington, DC in a closed long narrow zone between the Atlantic Ocean and the Appalachian Mountains. Some spatial agglomerations are unstable and transient but several spatial agglomerations that develop and prosper stably exist worldwide. Nowadays downtowns are revitalized through investment in transportation.

It is desirable to know what kinds of stable economic agglomeration patterns exist in two-dimensional economic space. Yet there may be a widespread pessimism that such stable equilibria are literally infinite and, therefore, cannot be exhausted. In this paper, to rebuff this pessimism, two questions about existence and stability are considered:

- What kinds of agglomeration patterns do *exist* in two dimensions?
- Among these patterns, which are *stable*?

A key to answer these two questions is to distinguish spatial and microeconomic properties and, as well as, model dependent and independent properties in economic agglomeration. The former question is answered in relation to spatial properties that are model independent and the latter to microeconomic properties of individual models.[5]

[5] Anas (2004) [2] stated "Of course, when the number of cities or the geographic space itself is limited or asymmetric, then agglomeration can arise as an artifact of the constraints imposed by geography as demonstrated by numerous NEG models. This reveals that the central agglomeration force in the NEG is space itself and not the underlying economic relations."

A preliminary and mandatory step to answer these questions is another question: "What are suitable spatial platforms of spatial economic activities?" Several spatial platforms have been developed, including two-place economy, long narrow economy,[6] racetrack economy,[7] and lattice economy[8] (Fig. 1). Their geometries are simple to complex in this order, and there is a tradeoff that a more complex economy can accommodate more patterns at the expense of increased analytical task. The lattice economy is apparently capable of accommodating two-dimensional patterns but involves a large number of degrees of freedom. The two-place economy is too simple, despite its vital role in the development of NEG models. Other one-dimensional economies, such as the long narrow and racetrack economies, are believed to be capable of grasping some essential agglomeration properties. Evolution of a regular lattice on a racetrack economy was set forth by Fujita, Krugman, and Venables (1999b) [15], and a "highly regular hierarchical system *a la* Christaller" on a long narrow economy was observed by Fujita, Krugman, and Mori (1999a) [14]. Tabuchi and Thisse (2011) [36] studied the racetrack economy for a multi-industry model to produce Christaller-like spatial patterns. Yet studies of these spatial platforms have been conducted somewhat independently[9] and several agglomeration patterns have been observed fragmentarily. It would be desirable to possess a synthetic view of spatial patterns on these platforms.

Hexagonal distributions have been advanced as the most geometrically feasible forms of agglomeration in central place theory. Yet there is a criticism: Although "it [central place theory] is a powerful idea too good for being left as an obscure theory" (Fujita, Krugman, and Mori, 1999a [14]), this theory is based only on a normative and geometrical approach and is not derived from market equilibrium conditions. As an early attempt to provide central place theory with a microeconomic foundation, Eaton and Lipsey (1975, 1982) [9, 10] showed the

[6] The long narrow economy was used by Fujita and Mori (1997) [16], Mori (1977) [26], and Fujita, Krugman, and Mori (1999a) [14].

[7] Agglomeration patterns of the racetrack economy were studied by Krugman (1993) [24], Fujita, Krugman, and Venables (1999b) [15], Picard and Tabuchi (2010) [32], Ikeda, Akamatsu, and Kono (2012a) [18], and Akamatsu, Takayama, and Ikeda (2012) [1].

[8] The dynamics of an urban spatial structure on a square lattice was studied by Clarke and Wilson (1985) [7] and numerical simulation of settlement formation on a square lattice was achieved by Munz and Weidlich (1990) [28]. Stelder (2005) [33] conducted a simulation of agglomeration for cities in Europe using a grid of points.

[9] A rare comparative study of the long narrow economy and the racetrack economy was conducted by Mossay and Picard (2011) [27] in a continuous space.

existence of a hexagonal distribution of mobile production factors (e.g., firms and workers) by a partial equilibrium approach without referring to the stability of hexagonal agglomeration. The hexagonal lattice has come to be acknowledged as a discretized counterpart of the *infinite plain* in central place theory. Hexagonal agglomeration on this lattice (without boundary) for core–periphery models was found by bifurcation theory and its stability was investigated by numerical analysis.[10]

This paper aims to answer the aforementioned questions about the *choice* of pertinent spatial platform and the *existence* and the *stability* of agglomeration patterns in two-dimensional economic space. To begin with, in view of the foregoing study (Footnote 10), it would be a logical sequel to choose a hexagonal lattice as a spatial platform of economic activities that can accommodate extensive patterns ranging from hexagons to racetracks and long narrow patterns. In this paper, two kinds of hexagonal lattices with and without boundary are considered. There is a tradeoff that the former is suitable for theoretical study and the latter is more realistic.

The question of the *existence* of agglomeration patterns can be answered by the theoretical study of the hexagonal lattice without boundary. This study resort to only spatial properties, and, therefore, is endowed with much-desired model independency. Agglomeration patterns of interest, such as hexagons *a la* Christaller and Lösch for centralization, racetracks expressing de-centralization, long narrow patterns, are shown to exist as equilibria by bifurcation theory. Unlike the previous studies that focused on hexagons (Footnote10), patterns other than hexagons are also considered in this paper. Market areas of the first-level centers for stable equilibria are shown to take various shapes, such as triangles, diamonds, and trapezoids, in addition to hexagons in central place theory, thereby going beyond the scope of central place theory.

The hexagonal lattice with boundary has asymmetry (inhomogeneity) as places near the boundary are not as competitive as places near the center. This is a more realistic spatial platform due to the presence of the boundary, but lacks a theoretical background to describe its agglomeration behavior. To compromise this lack, this paper employs a basic strategy to describe and understand agglomeration characteristics of the lattice with boundary based on theoretical information drawn from the lattice without boundary.

[10] See Ikeda, Murota, and Akamatsu (2012b) [21], Ikeda and Murota (2014) [20], and Ikeda et al. (2014) [22].

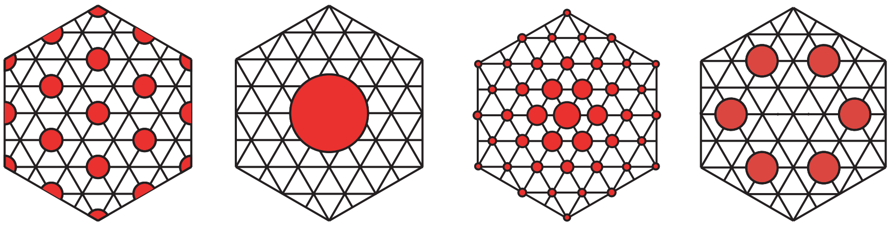

Figure 2: Agglomeration patterns of economic interest. Circles denote population size.

The answer to another question of the *stability* is dependent on models. While real economic activities allow models of various kinds, in order to deepen discussion on the stability, we refer to a specific economic geography model: Forslid and Ottaviano (2003) [12] version of modeling of Krugman (1991) [23].[11] When the transport cost is reduced from a large value, it is proved that the smallest hexagon (Fig. 2(a)) is the first non-uniform agglomeration pattern that breaks uniformity.[12] Although this proof is carried out for this specific model, it is extendable to a family of spatial economy models, for which the spatial interaction between places is distant decaying. By numerical comparative static analysis, the most likely stable progress of agglomeration patterns is shown as the formation of the smallest hexagon and gradual transition to patterns with larger market areas finally leading to an atomic mono-center en route to a megalopolis (Figs. 2(b) and (c)). Racetrack patterns (Fig. 2(d)), which are stable for very short durations, express the decay of the center of the domain (downtown), whereas hexagons are related downtown development.

This paper is organized as follows. Bifurcating agglomeration patterns for a two-dimensional economy are theoretically predicted in Section 2. Spatial economy models of interest are explained and the governing equation for the analytically solvable core–periphery model is presented in Section 3. Formulas for the value of transport cost at the emergence of downtown agglomeration are presented in Section 4. Stable agglomeration patterns in the hexagonal lattice without boundary are investigated numerically in Section 5 and the patterns in the lattice with boundary are examined in Section 6.

[11] There are two kinds of workers: unskilled workers are immobile and equally distributed along places, whereas skilled ones (footloose entrepreneurs) are mobile and choose the place to maximize wage. The immobile workers can be interpreted as a population attached to certain amenities.

[12] This proof is conducted by extending the strategy in Akamatsu, Takayama, and Ikeda (2012) [1], which utilizes the concept of spatial discounting.

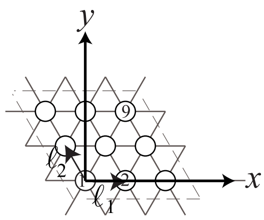

(a) 3×3 hexagonal lattice

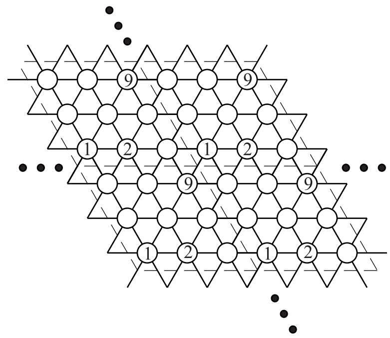

(b) Spatially repeated 3×3 hexagonal lattices

Figure 3: A system of places on a 3×3 hexagonal lattice with periodic boundary.

2. Bifurcating hexagons on a hexagonal lattice without boundary

In this paper, spatial properties and microeconomic properties are highlighted as independent sources of spatial agglomeration (Footnote 5). In this section, spatial properties, which are model independent, are studied.

A hexagonal lattice without boundary, which serves as a discretized counterpart of the isotropic infinite plain in central place theory, is introduced as a two-dimensional spatial platform suited for theoretical treatment. Possible bifurcating patterns on a hexagonal lattice without boundary are classified as a summary and reorganization of the theoretical studies of Lösch's hexagons (Ikeda and Murota, 2014 [20]; and Ikeda et al., 2014 [22]). In addition to these hexagons, we advance patterns of economic interest related to central place formation, de-centralization leading to decay of downtown, and formation of megalopolis.

Lösch's hexagons on a hexagonal lattice without boundary are introduced in Section 2.1. General form of spatial equilibrium conditions is presented in Section 2.2. Bifurcating hexagons are investigated in Section 2.3, and bifurcating equilibria are classified in Section 2.4.

2.1. Lösch's hexagons on a hexagonal lattice without boundary

As two-dimensional economic space, a hexagonal lattice comprising uniformly spread $n \times n$ places with periodic boundary[13] is considered (see Fig. 3(a) for $n = 3$). Goods are transported along the homogeneous transportation link of this lattice connecting neighboring places by roads of the same length.

[13] By virtue of this periodic boundary, this lattice can be repeated spatially to cover infinite two-dimensional space, and every place is linked to six hexagonal neighboring places (Fig. 3(b)).

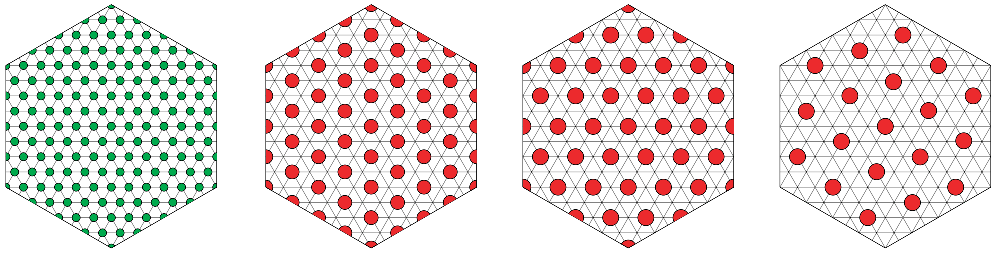

(a) $D = 1$ (flat earth) (b) $D = 3$ (c) $D = 4$ (d) $D = 7$

Figure 4: Lösch's hexagons on a hexagonal lattice. These patterns are obtained by spatially repeating $n \times n$ hexagonal lattices and cutting out hexagonal windows; circles represent the first-level places.

Lösch's hexagons (Lösch, 1940 [25]) were advanced as geometrically feasible agglomeration patterns in an infinite plain in central place theory. The spatial period L between spatially repeated hexagons takes some specific values, such as

$$L/l = \sqrt{D}, \quad D = 1, 3, 4, 7, 9, 12, 13, 16, 19, 21, 25, \ldots, \tag{1}$$

where l is the nominal distance between two neighboring places and $\sqrt{D}$ is proportional to the shortest Euclidean distance[14] between the first-level centers, i.e., the spatial period L of these centers. Figure 4 depicts some of these hexagons with $D = 1$, 3, 4, and 7. The smallest value $D = 1$ corresponds to the flat earth equilibrium (uniform distribution). The next three smallest values of $D = 3$, 4, and 7, respectively, are associated with Christaller's $k = 3$, 4, and 7 systems (Christaller, 1933 [6]).

2.2. General form of spatial equilibrium conditions

Although diverse spatial equilibrium models have been developed on the basis of an ensemble of economic principles and assumptions, it is possible to present a general form of spatial equilibrium. Let λ_i denote the population at the ith place, and define $\boldsymbol{\lambda} = (\lambda_1, \ldots, \lambda_K)^\top$, where K is the number of places, being equal to n^2 for the $n \times n$ hexagonal lattice.

The adjustment dynamics

$$\frac{d\boldsymbol{\lambda}(t)}{dt} = \boldsymbol{F}(\boldsymbol{\lambda}(t), \tau) \tag{2}$$

[14] In the application to spatial economy models (Section 3.2.1), the distance between places i and j for the transportation of goods on the hexagonal lattice is measured along the shortest link of the lattice. On the other hand, the spatial period L between neighboring first-level centers is measured by the Euclidean distance.

is considered with an appropriate function $\boldsymbol{F}(\boldsymbol{\lambda}, \tau)$ in $\boldsymbol{\lambda}$ and some parameter τ. A stationary point of this adjustment dynamics (2) is defined as $\boldsymbol{\lambda}$ that satisfies the spatial equilibrium condition

$$\boldsymbol{F}(\boldsymbol{\lambda}, \tau) = \boldsymbol{0}. \tag{3}$$

The stability of solution $\boldsymbol{\lambda}$ to (3) and the occurrence of bifurcation can be investigated via eigenanalysis of the Jacobian matrix[15] $J(\boldsymbol{\lambda}, \tau) = \partial \boldsymbol{F}/\partial \boldsymbol{\lambda}$.

For spatial economy models with observer-independence,[16] the flat earth equilibrium

$$\boldsymbol{\lambda}^* = \frac{1}{n^2}(1, \dots, 1)^\top \tag{4}$$

exists on the hexagonal lattice for any value of the parameter τ and are preserved until bifurcation.

2.3. Bifurcating hexagons

Bifurcating equilibria from the flat earth equilibrium $\boldsymbol{\lambda}^*$ in (4) were studied theoretically to assess the emergence of Lösch's hexagons (Ikeda and Murota, 2014 [20]). These theoretical results are given below.

2.3.1. Lösch's hexagon with $D = 3$: simple example

Lösch's hexagon with $D = 3$, which plays the most important role in the present study, is investigated in detail as a simple example. This hexagon is associated with a bifurcation point with twice repeated zero eigenvalues of the Jacobian matrix $J(\boldsymbol{\lambda}, \tau)$. These eigenvalues are associated with two linearly independent eigenvectors. For the 6×6 hexagonal lattice, for example, the two eigenvectors are given explicitly as

$$\begin{aligned}
\boldsymbol{q}_1 &= \frac{1}{3\sqrt{2}}(\cos(2\pi(n_1 - 2n_2)/3) \mid n_1, n_2 = 0, \dots, 5) \\
&= \frac{1}{6\sqrt{2}}(2\ {-1}\ {-1}\ 2\ {-1}\ {-1} \quad {-1}\ {-1}\ 2\ {-1}\ {-1}\ 2 \quad {-1}\ 2\ {-1}\ {-1}\ 2\ {-1} \\
&\qquad 2\ {-1}\ {-1}\ 2\ {-1}\ {-1} \quad {-1}\ {-1}\ 2\ {-1}\ {-1}\ 2 \quad {-1}\ 2\ {-1}\ {-1}\ 2\ {-1})^\top,
\end{aligned}$$

[15] The solution is termed linearly stable if every eigenvalue of the Jacobian matrix $J(\boldsymbol{\lambda}, \tau)$ has a negative real part, and linearly unstable if at least one eigenvalue has a positive real part. Bifurcation takes place when one or more eigenvalues become zero.

[16] The observer-independence is represented by the equivariance condition in nonlinear mathematics (e.g., Ikeda and Murota, 2010 [19]). This condition was proved for the core–periphery model (Section 3.2) in Ikeda, Murota, and Akamatsu (2012b) [21].

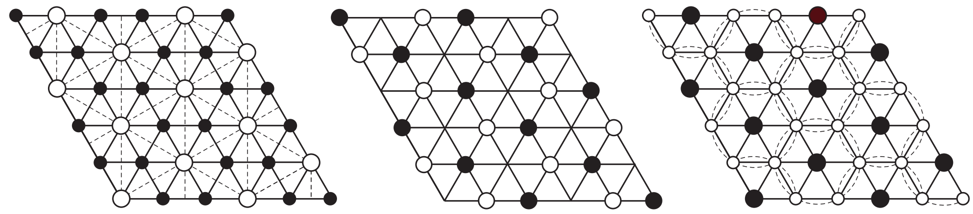

(a) $\boldsymbol{q}_1$ (hexagon with $D = 3$) (b) $\boldsymbol{q}_2$ (c) $-\boldsymbol{q}_1$ (racetrack)

Figure 5: Spatial patterns expressed by the vectors of $\boldsymbol{q}_1$, $\boldsymbol{q}_2$, and $-\boldsymbol{q}_1$ on the 6×6 hexagonal lattice. A white circle denotes a positive component and a black circle denotes a negative component.

$$
\begin{aligned}
\boldsymbol{q}_2 &= \frac{1}{3\sqrt{2}}(\sin(2\pi(n_1 - 2n_2)/3) \mid n_1, n_2 = 0, \dots, 5) \\
&= \frac{1}{6\sqrt{2}}(0 \ \ \sqrt{3} \ -\sqrt{3} \ \ 0 \ \ \sqrt{3} \ -\sqrt{3} \quad \sqrt{3} \ -\sqrt{3} \ \ 0 \ \ \sqrt{3} \ -\sqrt{3} \ \ 0 \quad -\sqrt{3} \ \ 0 \ \ \sqrt{3} \ -\sqrt{3} \ \ 0 \ \ \sqrt{3} \\
&\qquad\quad 0 \ \ \sqrt{3} \ -\sqrt{3} \ \ 0 \ \ \sqrt{3} \ -\sqrt{3} \quad \sqrt{3} \ -\sqrt{3} \ \ 0 \ \ \sqrt{3} \ -\sqrt{3} \ \ 0 \quad -\sqrt{3} \ \ 0 \ \ \sqrt{3} \ -\sqrt{3} \ \ 0 \ \ \sqrt{3})^{\top},
\end{aligned}
$$

where the coordinates are defined in accordance with Fig. 3. These eigenvectors are depicted in Figs. 5(a) and (b).

At the bifurcation point (repeated twice), the associated eigenvectors

$$c_1\boldsymbol{q}_1 + c_2\boldsymbol{q}_2$$

with constants c_1 and c_2 span a two-dimensional space. Bifurcating solutions of interest exist in the directions $\boldsymbol{q}_1$ and $-\boldsymbol{q}_1$. Herein, $\boldsymbol{q}_1$ represents Lösch's hexagon with $D = 3$, as shown by the dashed lines in Fig. 5(a), in which the first-level place with a white circle with increasing population is surrounded by six second-level places with black circles with decreasing populations. Vector $-\boldsymbol{q}_1$ represents a spatially-repeated racetrack pattern as depicted by the dashed circles in Fig. 5(c), in which the second-level place with decreasing population shown by (●) is surrounded by six first-level places with increasing populations shown by (○).

2.3.2. Lösch's hexagons: general issue

Theoretical results for these hexagons are summarized in the proposition below. Since smaller hexagons are of more economic interest, we focus hereafter on the five smallest hexagons with sizes $D = 3, 4, 7, 9$, and 12, as well as those with $D = 36$ appearing in the numerical analysis in Section 5.

Proposition 1. *Bifurcations from the flat earth equilibrium on the hexagonal lattice have the following properties:*

- *Property 1 (existence): Bifurcating equilibria associated with Lösch's hexagons with sizes* $D = 3, 4, 7, 9, 12$, *and* 36 *exist if and only if the size* n *of the lattice* *is equal, respectively, to*

$$n = \begin{cases} 3m, & \textit{for } D = 3 \textit{ and } D = 9, \\ 2m, & \textit{for } D = 4, \\ 7m, & \textit{for } D = 7, \\ 6m, & \textit{for } D = 12 \textit{ and } D = 36 \end{cases} \tag{5}$$

$(m = 1, 2, \ldots)$.

- *Property 2 (bifurcating patterns): Each of the bifurcating paths for Lösch's hexagons with sizes* $D = 3, 4, 7, 9, 12,$ *and* 36 *has a unique symmetry and this symmetry is preserved until further bifurcation takes place.*

2.4. Classification of bifurcating equilibria

Bifurcating equilibria are classified as a summary and extension of the theoretical analysis in Ikeda and Murota (2014) [20]. Bifurcation points are classified in accordance with the multiplicity M of the associated zero eigenvalues of the Jacobian matrix $J(\boldsymbol{\lambda}, \tau) = \partial \boldsymbol{F}/\partial \boldsymbol{\lambda}$ and the associated eigenvectors:

$$\boldsymbol{q}_1^{(k)}, \ldots, \boldsymbol{q}_M^{(k)} \tag{6}$$

with the correspondence between k and M given by[17]

k	1	3	4	7	9	36(I)	36(II)
M	1	2	3	12	6	6	12

(7)

Here the superscript (k) implies the size D of possible hexagons and there are two kinds of hexagons for $D = 36$, which are called $D = 36$(I) and $D = 36$(II). The eigenvectors in (6) are given by discrete Fourier series in two dimensions and their concrete forms are given in (A.3)–(A.9) in Appendix A.1.

The superposed eigenvectors

$$\sum_{i=1}^{M} c_i \boldsymbol{q}_i^{(k)}$$

for some constants $c_1, \ldots, c_M$ are possible candidates for the directions of bifurcating equilibria. By group-theoretic bifurcation analysis (Ikeda and Murota,

[17] In (7), the lattice size 7 is associated with $k = 1$ and 7 and the lattice size 6 with $k = 1, 3, 4, 9,$ 36(I), and 36(II).

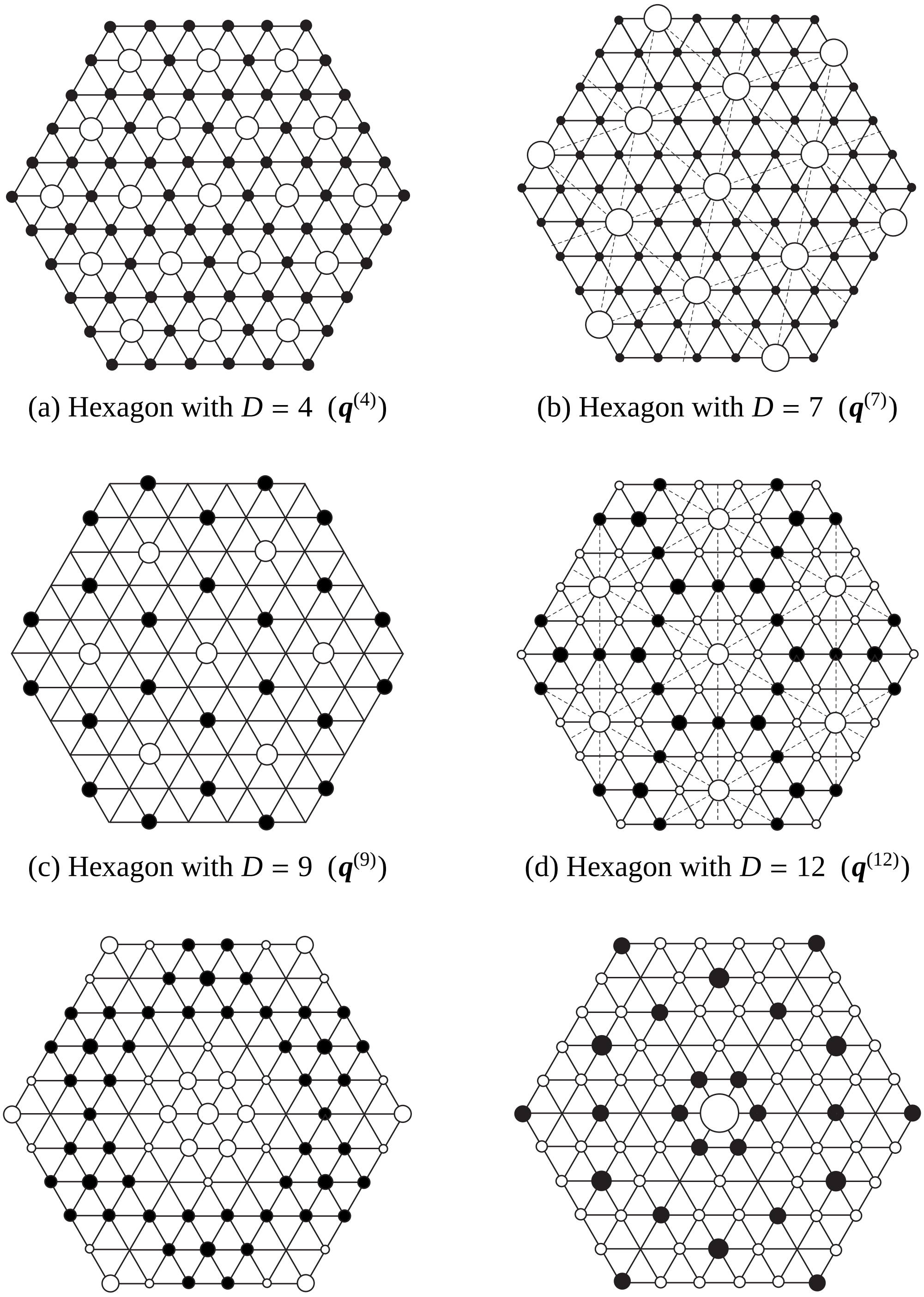

(a) Hexagon with $D = 4$ ($\boldsymbol{q}^{(4)}$)

(b) Hexagon with $D = 7$ ($\boldsymbol{q}^{(7)}$)

(c) Hexagon with $D = 9$ ($\boldsymbol{q}^{(9)}$)

(d) Hexagon with $D = 12$ ($\boldsymbol{q}^{(12)}$)

(e) Megalopolis with $D = 36$(I) ($\boldsymbol{q}^{(36(\mathrm{I}))}$)

(f) Megalopolis with $D = 36$(II) ($\boldsymbol{q}^{(36(\mathrm{II}))}$)

Figure 6: Hexagon and megalopolis patterns on a hexagonal window expressed by eigenvectors on 6×6 and 7×7 hexagonal lattices. These patterns are obtained by spatially repeating $n \times n$ hexagonal lattices and cutting out hexagonal windows; a white circle denotes a positive component and a black circle denotes a negative component.

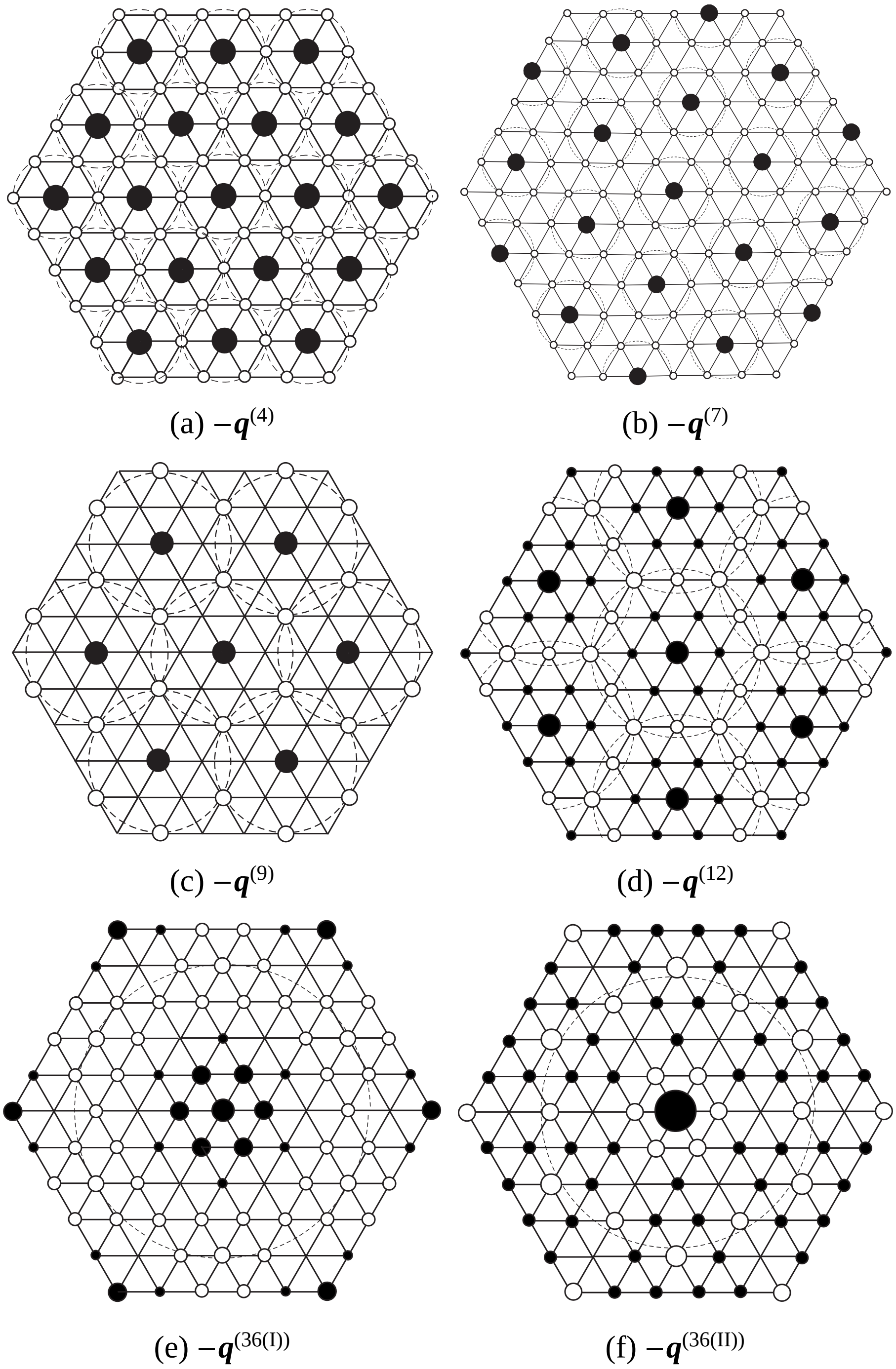

Figure 7: Racetrack patterns on hexagonal windows expressed by eigenvectors on 6×6 and 7×7 hexagonal lattices. A white circle denotes a positive component and a black circle denotes a negative component.

2014 [20]), the eigenvectors for the directions of hexagons for the 6×6 hexagonal lattice were obtained as

$$\begin{cases} \boldsymbol{q}^{(3)} = \boldsymbol{q}_1^{(3)}, \\ \boldsymbol{q}^{(4)} = \boldsymbol{q}_1^{(4)} + \boldsymbol{q}_2^{(4)} + \boldsymbol{q}_3^{(4)}, \\ \boldsymbol{q}^{(k)} = \boldsymbol{q}_1^{(k)} + \boldsymbol{q}_3^{(k)} + \boldsymbol{q}_5^{(k)}, \qquad k = 9, 12, 36(\mathrm{I}), \\ \boldsymbol{q}^{(36(\mathrm{II}))} = \boldsymbol{q}_1^{(36(\mathrm{II}))} + \boldsymbol{q}_3^{(36(\mathrm{II}))} + \boldsymbol{q}_5^{(36(\mathrm{II}))} + \boldsymbol{q}_7^{(36(\mathrm{II}))} + \boldsymbol{q}_9^{(36(\mathrm{II}))} + \boldsymbol{q}_{11}^{(36(\mathrm{II}))}, \end{cases} \tag{8}$$

which are given explicitly in (A.10)–(A.15) in Appendix A.1, whereas $\boldsymbol{q}^{(7)}$ can be consulted with Ikeda and Murota (2014,Chap.7) [20]. These hexagons are illustrated in Figs. 5(a) and 6.

There are possible bifurcating patterns of economic interest, which are beyond the scope of central place theory.[18]

- **Megalopolis patterns** are associated with eigenvectors: $\boldsymbol{q}^{(36(\mathrm{I}))}$ and $\boldsymbol{q}^{(36(\mathrm{II}))}$. As shown in Figs. 6(e) and (f), satellite places with small population are scattered around the center of the hexagonal window (downtown) to form a megalopolis. In particular, $\boldsymbol{q}^{(36(\mathrm{I}))}$ expresses a bump-shaped population distribution near the center expressing centralization.

- **Racetrack patterns** are associated with eigenvectors with the reversed sign:

$$-\boldsymbol{q}^{(k)}, \quad k = 3, 4, 7, 9, 12, 36(\mathrm{I}), 36(\mathrm{II}), \tag{9}$$

  which display racetracks of several kinds, which express de-centralization and are interpreted as the decay of downtown. For $D = 3, 4$, and 7, one place decaying into the second level center is surrounded by six places developing into the first level centers (Figs. 5(c) and 7(a),(b)). Semi-circular zones of growing places are observed for $D = 12, 36(\mathrm{I}), 36(\mathrm{II})$ (Figs. 7(d)–(f)).

- **Long narrow patterns** are given by the eigenvectors $\boldsymbol{q}_2^{(4)}$, $\boldsymbol{q}_3^{(9)}$, $\boldsymbol{q}_5^{(12)}$, and $\boldsymbol{q}_3^{(36(\mathrm{I}))}$. First-level places are located along spatially repeated narrow stripes and represent a chain of cities forming an industrial belt in a two-dimensional infinite space (Fig. 8).

- **Deformed hexagon** is associated with $\boldsymbol{q}_1^{(36(\mathrm{II}))}$ (Appendix A.2). The first-level places form spatially repeated deformed hexagons (Fig. 9).

[18]The existence of the deformed hexagon is proved in Appendix A.2 as a theoretical contribution of this paper, while the existence of hexagons, racetrack patterns, and long narrow patterns was proved in Ikeda and Murota (2014) [20].

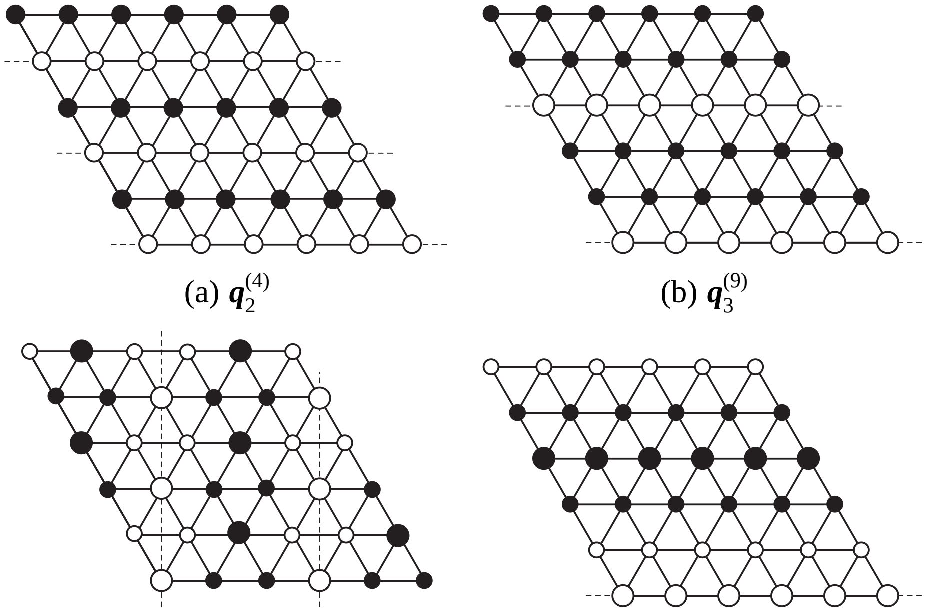

(a) $\boldsymbol{q}_2^{(4)}$ (b) $\boldsymbol{q}_3^{(9)}$

(c) $\boldsymbol{q}_5^{(12)}$ (d) $\boldsymbol{q}_3^{(36(\mathrm{I}))}$

Figure 8: Long narrow patterns on the hexagonal lattice expressed by eigenvectors on the 6×6 hexagonal lattice. A white circle denotes a positive component and a black circle denotes a negative component.

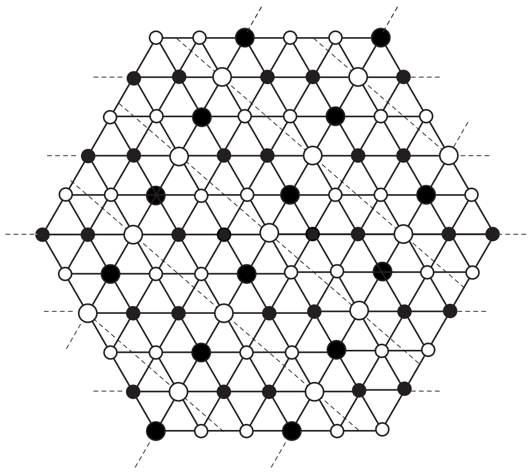

$\boldsymbol{q}_1^{(36(\mathrm{II}))}$

Figure 9: Deformed hexagon on the hexagonal window expressed by an eigenvector on the 6×6 hexagonal lattice. A white circle denotes a positive component and a black circle denotes a negative component.

3. Modeling of spatial economy

After the description of spatial properties in Section 2, modeling of spatial economy is presented in this section. After the explanation of a family of spatial economy models in Section 3.1, an analytically solvable core–periphery model that is put to use later in the analysis is presented in Section 3.2.

3.1. Spatial economy models

In many spatial economy models, the spatial interaction between places i and j is distance decaying and its effect is expressed by the spatial discounting factor d_{ij} representing the friction of distance,[19]

$$d_{ij} = r^{\,m(i,j)}, \tag{10}$$

where $m(i, j)$ is an integer proportional to the shortest distance between the places i and j, and r is a parameter satisfying $0 < r < 1$. With the use of a matrix form of d_{ij},

$$D = (d_{ij}), \tag{11}$$

the indirect utility (or profit) vector $\boldsymbol{v}$ is expressed

$$\boldsymbol{v} = \boldsymbol{v}(\boldsymbol{\lambda}, D), \tag{12}$$

where $\boldsymbol{\lambda}$ is the vector expressing distribution of population (or firms).

In social interaction models, r is given as a monotonically increasing function of the parameter τ expressing accessibility between places (see, e.g., Fujita and Ogawa, 1982 [17]; and Tabuchi, 1986 [34]).

In contrast, in NEG models (see, e.g., Oyama, 2009 [31]; and Akamatsu, Takayama, and Ikeda 2012 [1]), r is given as a monotonically decreasing function of the transport cost parameter τ satisfying

$$r(0) = 1, \quad r(+\infty) = 0.$$

Here $r(0) = 1$ represents the state of no transport cost and $r(+\infty) = 0$ means the state of infinite transport cost. When τ is decreased from a large value, the progress of agglomeration in population $\boldsymbol{\lambda}$ is studied by investigating the indirect utility function vector of the form (see Section 3.2.2)

$$\hat{\boldsymbol{v}}(\boldsymbol{\lambda}, \tau) = \boldsymbol{v}(\boldsymbol{\lambda}, D(r(\tau))). \tag{13}$$

[19] The present discussion is applicable with minor modifications to models using a linear transport cost (e.g., Beckmann, 1976 [4]; Ottaviano, Tabuchi, and Thisse, 2002 [30]; and Mossay and Picard, 2011 [27]).

It is proved in Section 4 for a hexagonal lattice without boundary and a spatial economy model (Section 3.2) that the flat earth equilibrium is stable for a very large τ ($\to +\infty$) and that, when τ is reduced from $+\infty$, the agglomeration pattern breaking uniformity is the smallest hexagon with $D = 3$.

3.2. *Core–periphery model*

As a representative of spatial economy models, an analytically solvable core–periphery model by Forslid and Ottaviano (2003) [12] is employed, whereas the methodology presented in this paper, in principle, is applicable to other models. The fundamental logic and governing equation of this model, which replaces the production function of Krugman with that of Flam and Helpman (1987) [11], are presented.

3.2.1. *Basic assumptions*

The economy of this model is composed of K places (labeled $i = 1, \dots, K$), two factors of production (skilled and unskilled labor) and two sectors (manufacturing, M, and agriculture, A). Both H skilled and L unskilled workers consume two types of final goods: manufacturing sector goods and agricultural sector goods. Workers supply one unit of each type of labor inelastically. Skilled workers are mobile among places, and the number of skilled workers in place i is denoted by λ_i ($\sum_{i=1}^{K} \lambda_i = H$). The total number H of skilled workers is normalized as $H = 1$. Unskilled workers are immobile and equally distributed across all places with unit density (i.e., $L = 1 \times K$).

Preferences U over the M- and A-sector goods are identical across individuals. The utility of an individual in place i is

$$U(C_i^{\mathrm{M}}, C_i^{\mathrm{A}}) = \mu \log C_i^{\mathrm{M}} + (1-\mu) \log C_i^{\mathrm{A}} \qquad (0 < \mu < 1), \tag{14}$$

where μ is a constant parameter expressing the expenditure share of manufacturing sector goods, C_i^{A} is the consumption of the A-sector product in place i, and C_i^{M} is the manufacturing aggregate in place i, which is defined as

$$C_i^{\mathrm{M}} \equiv \left(\sum_j \int_0^{n_j} q_{ji}(\ell)^{(\sigma-1)/\sigma} d\ell \right)^{\sigma/(\sigma-1)},$$

where $q_{ji}(\ell)$ is the consumption in place i of a variety $\ell \in [0, n_j]$ produced in place j, n_j is the number of available varieties, and $\sigma > 1$ is the constant elasticity of substitution between any two varieties. The budget constraint is given as

$$p_i^{\mathrm{A}} C_i^{\mathrm{A}} + \sum_j \int_0^{n_j} p_{ji}(\ell) q_{ji}(\ell) d\ell = Y_i, \tag{15}$$

where p_i^{A} is the price of A-sector goods in place i, $p_{ji}(\ell)$ is the price of a variety ℓ in place i produced in place j and Y_i is the income of an individual in place i. The incomes (wages) of skilled workers and unskilled workers are represented, respectively, by w_i and w_i^{L}.

An individual in place i maximizes the utility in (14) subject to the budget constraint in (15). This yields the following demand functions:

$$C_i^{\mathrm{A}} = (1-\mu)\frac{Y_i}{p_i^{\mathrm{A}}}, \quad C_i^{\mathrm{M}} = \mu\frac{Y_i}{\rho_i}, \quad q_{ji}(\ell) = \mu\frac{\rho_i^{\sigma-1}Y_i}{p_{ji}(\ell)^{\sigma}}, \tag{16}$$

where ρ_i denotes the price index of the differentiated products in place i, which is

$$\rho_i = \left(\sum_j \int_0^{n_j} p_{ji}(\ell)^{1-\sigma} d\ell\right)^{1/(1-\sigma)}. \tag{17}$$

Since the total income and population in place i are $w_i\lambda_i + w_i^{\mathrm{L}}$ and $\lambda_i + 1$, respectively, we have the total demand $Q_{ji}(\ell)$ in place i for a variety ℓ produced in place j:

$$Q_{ji}(\ell) = \mu\frac{\rho_i^{\sigma-1}}{p_{ji}(\ell)^{\sigma}}(w_i\lambda_i + w_i^{\mathrm{L}}), \tag{18}$$

The A-sector is perfectly competitive and produces homogeneous goods under constant-returns-to-scale technology, which requires one unit of unskilled labor in order to produce one unit of output. For simplicity, we assume that the A-sector goods are transported between places without transportation cost and that they are chosen as the numéraire. These assumptions mean that, in equilibrium, the wage of an unskilled worker w_i^{L} is equal to the price of A-sector goods in all places (i.e., $p_i^{\mathrm{A}} = w_i^{\mathrm{L}} = 1$ for each $i = 1, \ldots, K$).

The M-sector output is produced under increasing-returns-to-scale technology and Dixit-Stiglitz monopolistic competition. A firm incurs a fixed input requirement[20] of α units of skilled labor and a marginal input requirement of β units of unskilled labor. That is, a linear technology in terms of unskilled labor is assumed in the profit function. Given the fixed input requirement α, the skilled labor market clearing implies $n_i = \lambda_i/\alpha$ in equilibrium. An M-sector firm located in place i chooses $(p_{ij}(\ell) \mid j = 1, \ldots, K)$ that maximizes its profit

$$\Pi_i(\ell) = \sum_j p_{ij}(\ell)Q_{ij}(\ell) - (\alpha w_i + \beta x_i(\ell)),$$

[20]Given the fixed input requirement α, the skilled labor market clearing implies $n_i = \lambda_i/\alpha$ in equilibrium.

where $x_i(\ell)$ is the total supply.[21]

The transportation costs for M-sector goods are assumed to take the iceberg form. That is, for each unit of M-sector goods transported from place i to place j ($\neq i$), only a fraction $1/T_{ij} < 1$ actually arrives ($T_{ii} = 1$). More concretely, the transport cost T_{ij} between places i and j is defined as

$$T_{ij} = \exp(\tau\, m(i, j)\, \tilde{L}), \tag{19}$$

where τ is the transport cost parameter and $\tilde{L}$ is the nominal distance, which is chosen as $1/n$ for the $n \times n$ hexagonal lattice. (We define $T_{ii} = 1$.) Consequently, the total supply $x_i(\ell)$ is given as $x_i(\ell) = \sum_j T_{ij} Q_{ij}(\ell)$.

Since we have a continuum of firms, each firm is negligible in the sense that its action has no impact on the market (i.e., the price indices). Therefore, the first-order condition for profit maximization yields

$$p_{ij}(\ell) = \frac{\sigma\beta}{\sigma - 1} T_{ij}. \tag{20}$$

This expression implies that the price of the M-sector products does not depend on variety ℓ, so that $Q_{ij}(\ell)$ and $x_i(\ell)$ do not depend on ℓ. Therefore, argument ℓ is suppressed in the sequel. Substituting (20) into (17), we have the price index

$$\rho_i = \frac{\sigma\beta}{\sigma - 1} \left(\frac{1}{\alpha} \sum_j \lambda_j d_{ji} \right)^{1/(1-\sigma)}, \tag{21}$$

where

$$d_{ji} = T_{ji}^{1-\sigma} \tag{22}$$

is a spatial discounting factor between places j and i; d_{ji} is obtained as $(p_{ji} Q_{ji})/(p_{ii} Q_{ii})$ with (18) and (20), which means that d_{ji} is the ratio of total expenditure in place i for each M-sector product produced in place j to the expenditure for a domestic product. With the use of (19) and (22), r in (10) is related to τ by

$$r = \exp[-\tau(\sigma - 1)\tilde{L}]. \tag{23}$$

We have $0 < r < 1$ for $\tau > 0$

3.2.2. Market equilibrium

In the short run, skilled workers are immobile between places, i.e., their spatial distribution $\boldsymbol{\lambda} = (\lambda_i)$ is assumed to be given. The market equilibrium conditions

[21]The function $(\alpha w_i + \beta x_i(\ell))$ is the cost function by Flam and Helpman (1987) [11].

consist of the M-sector goods market clearing condition and the zero-profit condition because of the free entry and exit of firms.

The market equilibrium wage $w_i(\boldsymbol{\lambda}, \tau)$ is determined by the equation (see, Akamatsu, Takayama, and Ikeda, 2012 [1])

$$w_i(\boldsymbol{\lambda}, \tau) = \frac{\mu}{\sigma} \sum_{j=1}^{K} \frac{d_{ij}}{\Delta_j(\boldsymbol{\lambda}, \tau)} (w_j(\boldsymbol{\lambda}, \tau)\lambda_j + 1). \tag{24}$$

Here, $\Delta_j(\boldsymbol{\lambda}, \tau) = \sum_{k=1}^{K} d_{kj}\lambda_k$ denotes the market size of the M-sector in place j. The indirect utility $v_i(\boldsymbol{\lambda}, \tau)$, given the spatial distribution of the skilled workers, is obtained as

$$v_i(\boldsymbol{\lambda}, \tau) = \frac{\mu}{\sigma - 1} \log \Delta_i(\boldsymbol{\lambda}, \tau) + \log[w_i(\boldsymbol{\lambda}, \tau)]. \tag{25}$$

The equation (24) is solvable for w_i as follows. We set

$$\begin{cases} \boldsymbol{w} = (w_i), \quad D = (d_{ij}), \quad \Delta = \mathrm{diag}(\Delta_1, \dots, \Delta_K), \\ \Lambda = \mathrm{diag}(\lambda_1, \dots, \lambda_K), \quad \mathbf{1} = (1, \dots, 1)^\top. \end{cases} \tag{26}$$

Then (24) becomes

$$\boldsymbol{w} = \frac{\mu}{\sigma} D\Delta^{-1}(\Lambda\boldsymbol{w} + \mathbf{1}),$$

which is solvable with respect to $\boldsymbol{w}$ as

$$\boldsymbol{w} = \frac{\mu}{\sigma} \left(I - \frac{\mu}{\sigma} D\Delta^{-1}\Lambda\right)^{-1} D\Delta^{-1}\mathbf{1}.$$

Then the use of this equation in (25) gives the indirect utility function vector $\boldsymbol{v} = \boldsymbol{v}(\boldsymbol{\lambda}, \tau)$ (cf., (13)).

3.2.3. Spatial equilibrium conditions

In the description of spatial (long-run) equilibrium of the economic state for mobile workers, we assume a specific functional form

$$\boldsymbol{F}(\boldsymbol{\lambda}, \tau) = H\boldsymbol{P}(\boldsymbol{v}(\boldsymbol{\lambda}, \tau)) - \boldsymbol{\lambda} \tag{27}$$

of the governing equation (3). Here, $\boldsymbol{P}(\boldsymbol{v}) = (P_1, \dots, P_K)^\top$ is the choice function vector that satisfies $\sum_{i=1}^{K} P_i = 1$. We have $H = 1$, as a normalization.

As the choice function, we employ the logit choice function[22] $P_i = P_i(\boldsymbol{v})$ given by

$$P_i(\boldsymbol{v}) = \frac{\exp(\theta v_i)}{\sum_{j=1}^{K} \exp(\theta v_j)}, \tag{28}$$

[22]The skilled workers are assumed to be heterogeneous in their preferences for location choice (e.g., Tabuchi and Thisse, 2002 [35]; Murata, 2003 [29]).

where θ is a positive parameter.[23] The adjustment process described by (2) with (27) and (28) is the logit dynamics (e.g., Fudenberg and Levine, 1998 [13]).

[23] Parameter θ in (28) denotes the inverse of variance of the idiosyncratic taste, which is assumed to follow the Gumbel distribution that is identical across places (e.g., Anderson, de Palma, and Thisse, 1992 [3]). In the limit of $\theta \to \infty$, this form reduces to the standard replicator dynamics.

4. Break point triggering spatial agglomeration

For the two-place economy, the *break point* of the transport cost τ, at which symmetric places change catastrophically into a core–periphery pattern, is highlighted as a key concept (Fujita, Krugman, and Venables, 1999 [15]). For the hexagonal lattice, break points for Lösch's hexagons leading to centralization are of most economic interest. In this section, these break points are investigated by exploiting both spatial properties and microeconomic properties. Major results are presented, while details of derivation are given in Appendix B.

The analytically solvable core–periphery model is employed (Section 3.2) and the size n of the lattice is chosen as $n = 6$ so as to encompass hexagons with various sizes ($D = 3, 4, 9, 12, 36(\mathrm{I}), 36(\mathrm{II})$) (cf., Proposition 1 in Section 2.3.2). Nonetheless, the methodology employed herein is general and is extendable to other spatial economy models (Section 3.1) and to the hexagonal lattice for any size n.

Theoretical formulas for the break points are derived in Section 4.1, and the order of emerging hexagons is studied in Section 4.2.

4.1. Laws for break point

When the transport cost parameter τ is reduced continuously from $+\infty$ to 0, two break points are encountered for each hexagon under certain conditions on the values of μ, σ and θ for $n = 6$.

Proposition 2. *For each Lösch's hexagon, two break points τ_+ and τ_- with $\tau_+ > \tau_- > 0$ exist when the following conditions*[24] *are satisfied:*

$$\frac{\mu}{\sigma - 1} < 1 + \theta^{-1}, \tag{29}$$

$$\mu^2 \left[\frac{1}{\sigma}(1 + \theta^{-1}) + \frac{1}{\sigma - 1} \right]^2 - 4\theta^{-1} \left(\frac{\mu^2}{\sigma(\sigma - 1)} + 1 \right) > 0. \tag{30}$$

Since these conditions for the existence of break points are common for all hexagons with $D = 3, 4, 9, 12, 36(\mathrm{I}), 36(\mathrm{II})$, the violation of either of these conditions leads to the disappearance of all hexagons. This is the worst case scenario in downtown development through social investment in that no agglomeration emerges at whatever cost.

A formula for the break points is given below.

[24] In the limit of $\theta \to \infty$ (Footnote 23), the second condition (30) is always satisfied and the first condition (29) reduces to the no-black-hole condition $\mu/(\sigma - 1) < 1$ in Forslid and Ottaviano (2003) [12].

Proposition 3. *Break points $\tau_+^{(k)}$ and $\tau_-^{(k)}$ for Lösch's hexagon with the size k are given by*

$$\tau_+^{(k)} = -\frac{6}{\sigma - 1}\log(\Phi^{(k)}(\epsilon_+^*)), \quad \tau_-^{(k)} = -\frac{6}{\sigma - 1}\log(\Phi^{(k)}(\epsilon_-^*)),$$
$$k = 3, 4, 9, 12, 36(\mathrm{I}), 36(\mathrm{II}). \tag{31}$$

Here,

$$\epsilon_+^* = \frac{b + \sqrt{b^2 - 4a\theta^{-1}}}{2a}, \quad \epsilon_-^* = \frac{b - \sqrt{b^2 - 4a\theta^{-1}}}{2a}$$

with

$$a = \frac{\mu^2}{\sigma(\sigma - 1)} + 1, \quad b = \frac{\mu}{\sigma}(1 + \theta^{-1}) + \frac{\mu}{\sigma - 1},$$

and $r = \Phi^{(k)}(\epsilon)$ is a function defined implicitly from the relation

$$\epsilon = \frac{\tilde{\epsilon}^{(k)}(r)}{1 + 6r + 12r^2 + 15r^3 + 2r^4}, \qquad k = 3, 4, 9, 12, 36(\mathrm{I}), 36(\mathrm{II}),$$

where

$$\tilde{\epsilon}^{(k)}(r) = \begin{cases} 1 - 3r + 3r^2 - 3r^3 + 2r^4 & \text{for } k = 3, \\ 1 - 2r + 4r^2 - 5r^3 + 2r^4 & \text{for } k = 4, \\ 1 - 3r^2 + 3r^3 - r^4 & \text{for } k = 9, \\ 1 + r - 5r^2 + r^3 + 2r^4 & \text{for } k = 12, \\ 1 + 4r + r^2 - 5r^3 - r^4 & \text{for } k = 36(\mathrm{I}), \\ 1 - 2r + r^2 + r^3 - r^4 & \text{for } k = 36(\mathrm{II}). \end{cases}$$

Although the formula (31) is rigorous, the following approximate formula is more convenient in the discussion of parameter dependence of the break point for Lösch's hexagon with $D = 3$.

Proposition 4. *Under the conditions*

$$\theta \gg (\sigma/\mu)^2 \gg 1, \tag{32}$$

the larger break point $\tau_+^{(3)}$ for Lösch's hexagon with $D = 3$ is given approximately as

$$\tau_+^{(3)} = 18 \cdot 2^{1/3}\,\frac{\mu^{1/3}}{(\sigma - 1)^{4/3}}. \tag{33}$$

The approximate formula (33) indicates that the onset of agglomeration is accelerated by a lower substitution σ between any two varieties and a higher expenditure share μ of manufactured goods. This is in line with economic intuition and the present numerical examples in Sections 5.4 and 6.2.

4.2. Order of emerging hexagons

As we have seen in Section 2, there are several bifurcations engendering hexagons of various kinds. The first bifurcation engendering a hexagon, when τ is reduced from a large value, is an important bifurcation breaking uniformity. In contrast, the last bifurcation is another important one related to a mature stage of economic agglomeration. It is possible to predetermine the order of the emergence of hexagons as expounded in the following proposition, which is applicable to a family of spatial economy models introduced in Section 3.1.

Proposition 5. *The flat earth equilibrium is stable for a large* τ $(> \tau_+^{(3)})$*. When* τ *is reduced continuously from* $+\infty$ *to* 0 *[or* r *is increased continuously from* 0 *to* 1*] and bifurcations take place, these bifurcations occur in the following order.*

(i) Bifurcation producing Lösch's hexagon with $D = 3$ *occurs first at* $\tau = \tau_+^{(3)}$*.*

(ii) Bifurcation producing the megalopolis with $D = 36(\mathrm{I})$ *occurs last at* $\tau = \tau_-^{(36(\mathrm{I}))}$*.*

The smallest hexagon with $D = 3$ is the most important one that breaks the uniformity. It is no wonder that this hexagon was highlighted as Christaller's $k = 3$ system. Another hexagon with $D = 36(\mathrm{I})$, which is beyond the scope of central place theory, is also important as this hexagon comes at the tail of agglomeration expressing centralization leading to a megalopolis.[25]

[25]This megalopolis formation is inherent for the logit dynamics employed herein, but is absent for the replicator dynamics.

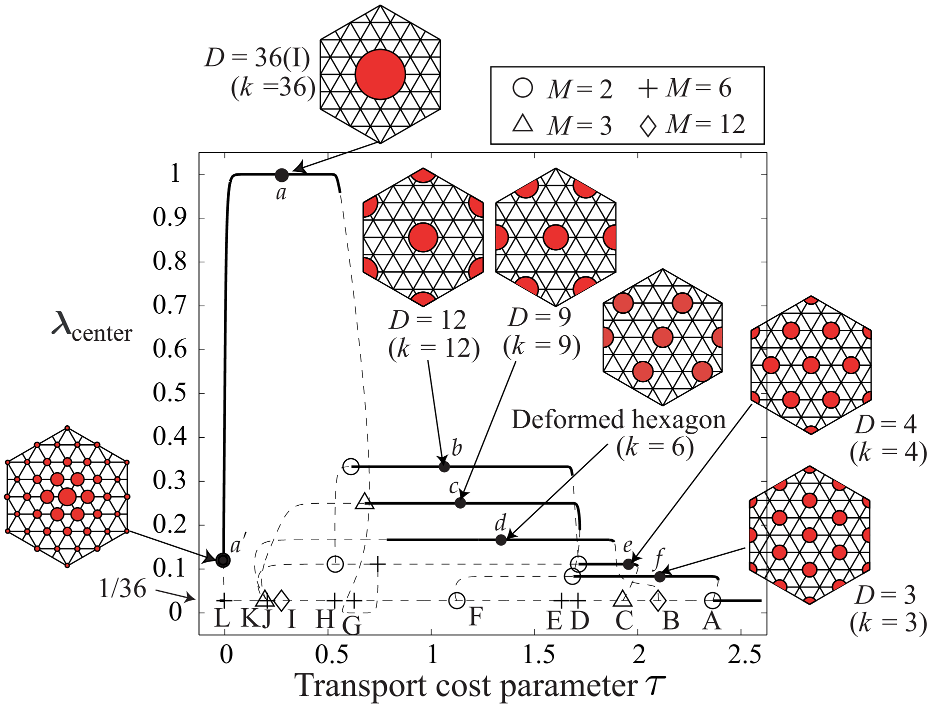

Figure 10: Equilibrium curves related to hexagons and associated population distributions displayed in the hexagonal windows containing 36 places. Solid curves represent stable equilibria and dashed ones represent unstable ones.

5. Stable agglomeration patterns on a hexagonal lattice without boundary

Using theoretically possible agglomeration patterns presented in Section 2.4, this section tackles the main objective of this paper to elucidate which patterns are stable and, therefore, of economic interest. For this purpose, equilibria of the 6×6 hexagonal lattice are studied by comparative static analysis with respect to the transport cost of the core–periphery model of Forslid and Ottaviano (2003) [12] (Section 3.2). Stable equilibria related to central place formation, decentralization leading to decay of downtown, and formation of megalopolis are shown to exist.

Stable bifurcating equilibria are observed in Section 5.1, and progress of stable equilibria under decreasing transport costs is studied in Section 5.2. Market areas of the first-level places are investigated in Section 5.3, and robustness of the progress of stable equilibria against parameter values is confirmed computationally in Section 5.4.

The distance between two neighboring places is chosen as $l = 1/6$. Parameter values are chosen as $(\sigma, \mu) = (5.0, 0.4)$, as in Fujita, Krugman, and Venables, 1999b [15]. The parameter θ in (28) is chosen as $\theta = 1000$ and the fixed input requirement is chosen as $\alpha = 1.0$. This set of parameter values satisfies the conditions (29) and (30) for the existence of break points.

5.1. Bifurcating stable equilibria

The flat earth equilibrium $\boldsymbol{\lambda} = \frac{1}{36}(1, \ldots, 1)^\top$ in (4) exist for any value of the transport cost parameter τ. This equilibrium is shown as the horizontal line $\lambda_{\text{center}} = 1/36$ in the equilibrium curves in Fig. 10, which plots the relations between the transport cost parameter τ and the population λ_{center} of the place at the center of the hexagonal window. There exist bifurcation points A through L on the equilibrium.[26]

Bifurcating equilibria branching from these bifurcation points are found with reference to the theoretical prediction in Section 2.4. Bifurcating hexagons are shown in Fig. 10, whereas stable bifurcating equilibria other than hexagons are summarized in Appendix C. Stable population distributions found in this manner are shown in Fig. 11 using the hexagonal window containing 36 places. The place at the center of this window can be interpreted as the downtown of a city area and, accordingly, the progress of agglomeration at this place is of most economic interest.

Durations of the transport cost parameter τ for stable equilibria are depicted in Fig. 12, in which the ordinate N_{1st} means the number of the first-level places (with the largest population). When τ is reduced, the number N_{1st} tends to be reduced and, in turn, to expand the market area. This is due to a trade-off between transportation cost and scale economies.[27]

The *hexagons* with $D = 3$, 4, 9, and 12 become stable in this order as τ decreases from a large value. Thus, these hexagons play an important role in the progress of centralized agglomeration, thereby showing the foresight of central place theory, which proposed these hexagons by the geometrical consideration.

In contrast, there are other stable patterns introduced below, which have not been obtained in central place theory, but are found by bifurcation theory (Section 2).

- **Megalopolis** (point a′ in Fig. 10) and *atomic mono-center* (point a) associated with the hexagon with $D = 36$(I) become stable for small τ.

- **Racetrack patterns** with $D = 12$ and $D = 36$ (Figs. 11(g) and (h)) are stable for very short ranges of the transport cost parameter ($1.71 < \tau < 1.74$

[26]The existence of bifurcations on the flat earth equilibrium is investigated by the eigenanalysis of the Jacobian matrix $J(\boldsymbol{\lambda}, \tau) = \partial \boldsymbol{F}/\partial \boldsymbol{\lambda}$ (Footnote 15).

[27]Firms at a place with a small market area enjoy the merit of a reduction of transportation cost at the expense of small scale economies. In contrast, firms at a place with a large market area enjoy the merit of scale economies at the expense of large transportation cost.

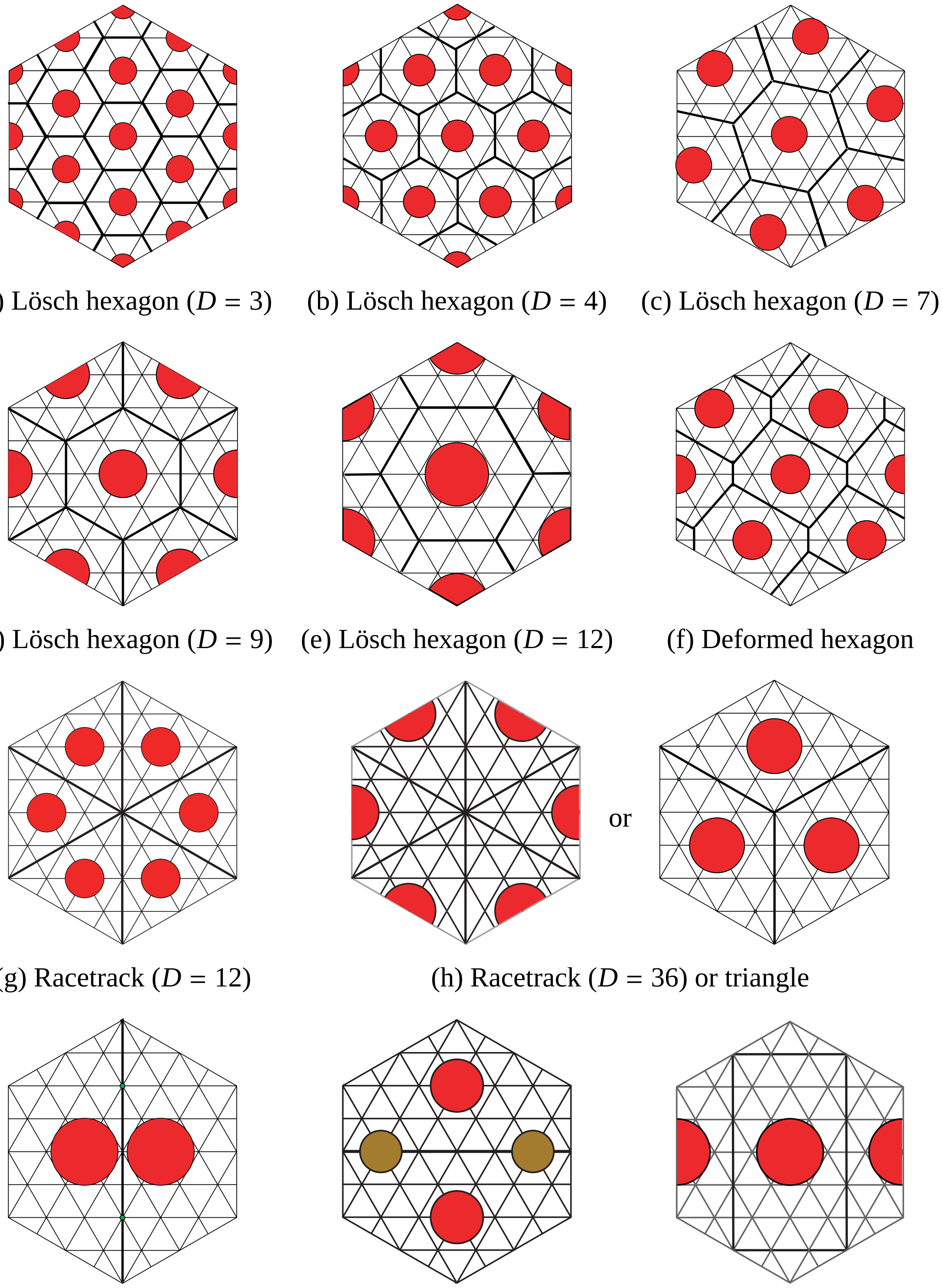

(a) Lösch hexagon (D = 3)
(b) Lösch hexagon (D = 4)
(c) Lösch hexagon (D = 7)
(d) Lösch hexagon (D = 9)
(e) Lösch hexagon (D = 12)
(f) Deformed hexagon
(g) Racetrack (D = 12)
(h) Racetrack (D = 36) or triangle
(i) Two places
(j) Semi-square
(k) Discrete long narrow pattern

Figure 11: Market areas of the first-level centers for stable equilibria. Lösch's hexagon with $D = 7$ in Fig. 11(c) does not exist on the 6×6 hexagonal lattice but is included here for comparison.

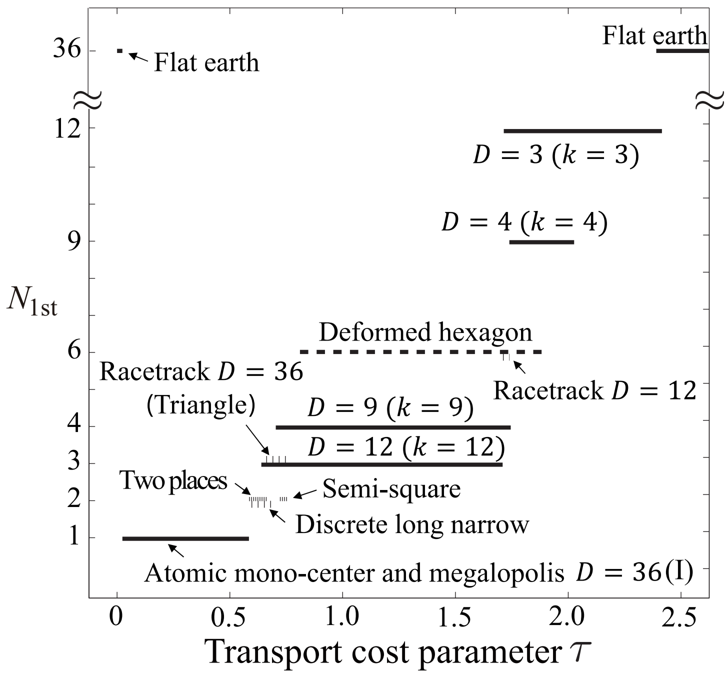

Figure 12: Durations of the transport cost parameter τ for stable equilibria. N_{1st} is the number of first-level places in the hexagonal window; a first-level place at the corner of the hexagonal window is counted as 1/3 and that at the midpoint of two neighboring corners is counted as 1/2 in the estimation of N_{1st}.

and $0.66 < \tau < 0.76$, respectively). These patterns are interpreted as decentralization leading to downtown decay or extinction and play a major role in the discussion of economic implications.

- **Deformed hexagon** (point d) is stable for a wide range $0.81 < \tau < 1.91$.
- **Two places and semi-square pattern** (Figs. 11(i) and (j)) have been found on the same curve of equilibrium.[28] Yet these two patterns are stable in very short ranges $0.59 < \tau < 0.67$ and $0.72 < \tau < 0.75$ and play a small role in the discussion on stable agglomeration.
- **Long narrow patterns** are unstable except for the discrete long narrow pattern shown in Fig. 11(k), which is stable for a short range $0.60 < \tau < 0.70$. Although these patterns resemble an industrial belt, such as the Atlantic seaboard of the United States, they would play a limited role in the agglom-

[28]The transition from the semi-square pattern to the two places (see Fig. C.3) is quite close to the one found in the racetrack economy, in which four identical first-level places were transformed into two identical places (Ikeda, Akamatsu, and Kono, 2012a [18]; and Akamatsu, Takayama, and Ikeda, 2012 [1]).

eration in wide two-dimensional space, such as southern Germany.

The hexagonal lattice without boundary employed herein can encompass several agglomeration features that have been observed fragmentarily in a long narrow economy (one-dimensional economy) as follows: Highly regular hierarchical system *a la* Christaller (Fujita, Krugman, and Mori, 1999a [14]), mono-center (Fujita and Mori, 1997 [16]; and Fujita, Krugman, and Mori, 1999a [14]), and megalopolis consisting of a continuous industrial zone around the center (Mori, 1997 [26]). However, there are still other stable equilibria, such as the racetrack, that cannot be deduced in one-dimensional economies but are found here for the hexagonal lattice.

5.2. *Progress of stable equilibria*

We now shift our attention to an issue of great economic interest, i.e., the progress of stable equilibria under decreasing transport costs. Possible progress is deduced from Fig. 12 as

$$
\begin{array}{ll}
\text{Dawn stage:} & \text{Flat earth} \Rightarrow \text{Hexagon } (D = 3) \Rightarrow \\
\text{Chaotic stage:} & \left\{ \begin{array}{l} \text{Hexagon } (D = 4) \\ \text{Racetrack } (D = 12) \\ \text{Deformed hexagon} \\ \text{Hexagon } (D = 9) \\ \text{Hexagon } (D = 12) \\ \text{Triangle} \\ \text{Racetrack } (D = 36) \\ \quad \vdots \end{array} \right\} \Rightarrow \\
\text{Mature stage:} & \text{Atomic mono-center} \Rightarrow \text{Megalopolis} \Rightarrow \text{Flat earth.}
\end{array}
\tag{34}
$$

Thus there are three major stages of agglomeration.

- **Dawn stage** is the one which was predicted by central place theory. When τ is reduced from a large value $\tau \approx 2.4$, the flat earth renders the role of the unique stable equilibrium to the hexagon with $D = 3$ ($\tau \approx 2.0$). Then a state of dual stable equilibria of the hexagons with $D = 3$ and $D = 4$ comes into existence ($1.7 < \tau < 2.0$).

- **Chaotic stage** goes beyond the scope of central place theory. When the hexagon with $D = 3$ becomes unstable at $\tau \approx 1.7$, there comes a state of multiple stable equilibria, such as hexagons with $D = 4$, 9, and 12, the racetracks, and the deformed hexagon. The existence of the stable racetrack patterns means that there is a possibility of the decay or extinction of the downtown.

- **Mature stage** is the final stage of economic agglomeration for a small τ, in which the atomic mono-center, the megalopolis, and the flat earth become stable in this order.

If only hexagons in central place theory were considered, progress of stable equilibria as τ decreases would lead to continuous progress of centralization through the increase of the size of hexagons (Fig. 10). This, however, is not a true scenario and there is a competition between centralization by hexagons and de-centralization by racetrack patterns. This demonstrates the importance of the present study, the scope of which goes beyond central place theory and encompasses diverse patterns other than hexagons.

5.3. Market areas of first-level places

The market areas depicted in Fig. 11 for stable equilibria display various shapes: hexagons, deformed hexagons, rectangles, diamonds, and trapezoids. In particular, Lösch's hexagons have superior stability in that they remain stable in wide ranges of τ (Fig. 12). Thus, these hexagons, which were advanced as geometrically superior shapes of market areas in central place theory, are also endowed with stability. The deformed hexagon with semi-hexagonal market areas also has superior stability. Other shapes, such as triangles, diamonds, and trapezoids are inferior in stability.

Let us briefly review central place theory. The ratio of the number k_1 of the first-level places to the number k_2 of the second-level places is a key concept in central place theory (Dicken and Lloyd, 1990 [8]), and is given by

$$k_1 : k_2 = 1 : (k-1) = \begin{cases} 1:2 & \text{for } D = 3\ (k=3), \\ 1:3 & \text{for } D = 4\ (k=4), \\ 1:6 & \text{for } D = 7\ (k=7). \end{cases} \tag{35}$$

This formula is extendible to other hexagons in Fig. 11 by setting $k = D$.

For the deformed hexagon, four second-level places are contained inside the market area of the first-level place and two second-level ones at the border are shared by two neighboring first-level places. Therefore, the ratio is given by

$$k_1 : k_2 = 1 : k - 1 = 1 : 5(= 4 + 2/2),$$

and the deformed hexagon can be interpreted as the $k = 6$ system in view of (35). A first-level place is connected to two first-level places by zigzag roads, as in the $k = 3$ system with market principle,[29] and to four first-level places by straight roads, as in the $k = 4$ system in line with traffic principle. This deformed hexagon is nearly endowed with the administrative principle of the $k = 7$ system because four among six second-level places are contained within the market area of the first-level place. Each first-level place is surrounded by six second-level places, as in the $k = 3$, $k = 4$, and $k = 7$ systems. Thus, the deformed hexagon is indeed a mixture of these three systems. This suffices to show the need for reconsideration of the framework of central place theory, even from a geometrical standpoint.

5.4. Robustness against parameter values

The robustness of the existence of stable equilibria is demonstrated against the change of the elasticity σ of substitution between any two varieties. Figure 13 shows durations of stable equilibria for $\sigma = 4.0$ and 10.0, where 5.0 is used as the standard value in this section. As σ decreases to 4.0 (Fig. 13(a)), not much difference is observed in comparison with Fig. 12 for the standard value. As σ increases to a large value of 10.0 and the economic balance shifts in favor of dispersion (Fig. 13(b)), the racetrack patterns become unstable. Yet the hexagons ($D = 3$, 4, 9, and 12), the deformed hexagon, the atomic mono-center, and the megalopolis all exist as stable equilibria. Moreover, when the transport cost decreases from a large value, the hexagon with $D = 3$ is formed first, followed by several stable equilibria, en route to the atomic mono-center, the megalopolis, and the flat earth. This suffices to demonstrate the robustness of the present discussion on stable equilibria.

[29] Christaller's $k = 3$, 4, and 7 systems correspond respectively to Lösch's hexagon with $D = 3$, 4, and 7.

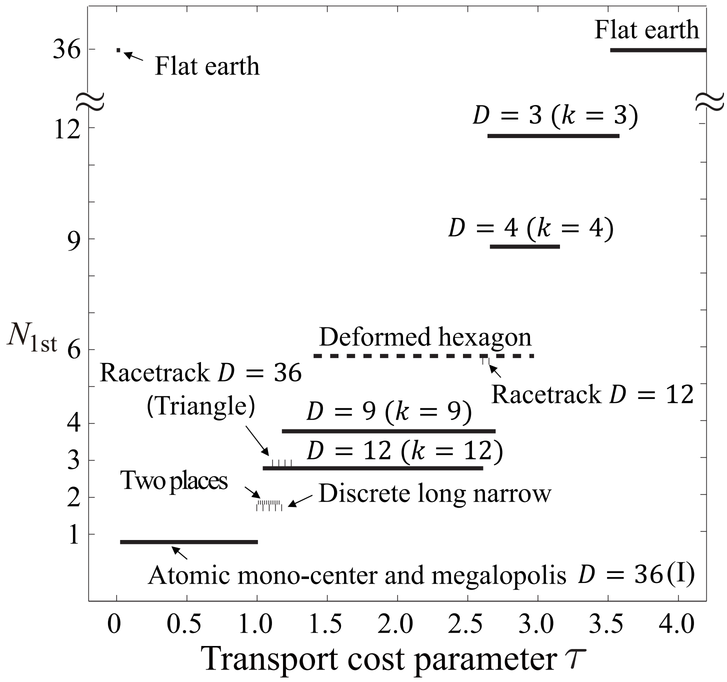

(a) $\sigma = 4.0$

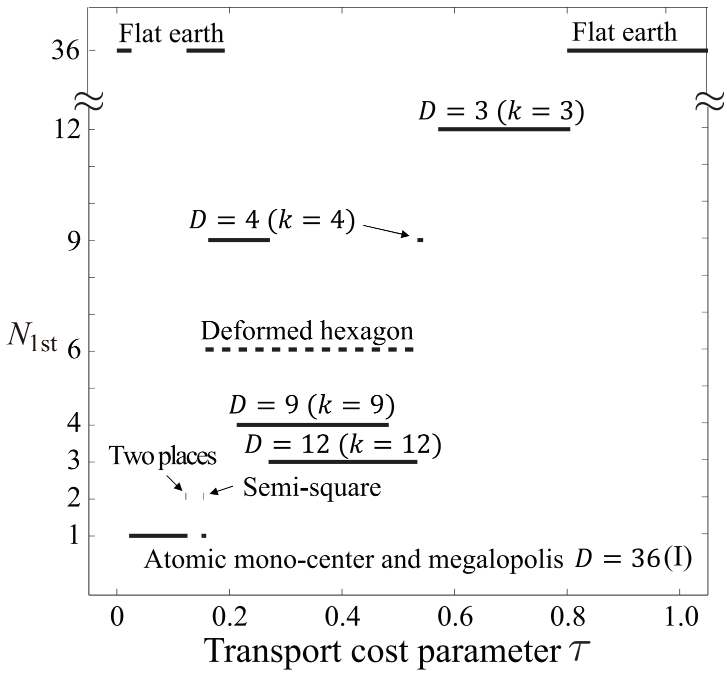

(b) $\sigma = 10.0$

Figure 13: Durations of the transport cost parameter τ for stable equilibria for several values of σ. N_{1st} is the number of first-level places in the hexagonal window; a first-level place at the corner of the hexagonal window is counted as 1/3 and that at the midpoint of two neighboring corners is counted as 1/2 in the estimation of N_{1st}.

6. Agglomeration patterns on a hexagonal lattice with boundary

The hexagonal lattice without boundary studied in Sections 2 and 5 realizes an infinite plain (homogeneous space) in central place theory and allows theoretical prediction of agglomeration patterns (Section 2.4). Yet there may be a criticism that a realistic economic space has a boundary which makes the space asymmetric. In this section, in search of realistic agglomeration patterns, we employ a hexagonal lattice with boundary in Fig. 14. Because places near border are not as competitive as places inside, this lattice has inhomogeneity (asymmetry) and theoretical prediction on agglomeration patterns is absent. In order to compensate for this absence, agglomeration of the lattice with boundary is described based on the theoretical prediction of the lattice without boundary in Section 2.

Progress of stable equilibria under decreasing transport costs is studied in Section 6.1. Parameter dependence is studied in Section 6.2.

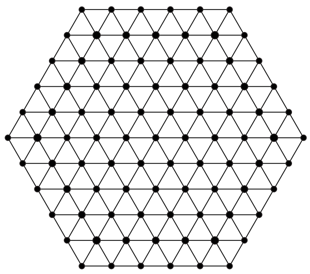

Figure 14: Hexagonal lattice with boundary with 91 places.

6.1. Progress of stable equilibria

Equilibrium curves and associated population distributions at points a to f shown in Fig. 15 for the lattice with boundary have been obtained for parameter values $(\sigma, \mu) = (5.0, 0.4)$ and $l = 1/6$, which are also used in Section 5. The stable equilibria progress as

$$\begin{array}{ll} \text{Dawn stage:} & \text{Flat earth} \Rightarrow \text{Hexagon } (D = 3) \Rightarrow \\ \text{Chaotic stage:} & \text{Hexagon } (D = 4) \Rightarrow \text{Racetrack } (D = 36) \Rightarrow \text{Hexagon } (D = 9) \Rightarrow \\ \text{Mature stage:} & \text{Atomic mono-center} \Rightarrow \text{Megalopolis} \Rightarrow \text{Flat earth.} \end{array} \tag{36}$$

As in the hexagonal lattice without boundary (Section 5), there are three stages.

- In the dawn stage ($\tau > 2.0$), after the flat earth equilibrium at point a, a hexagon with $D = 3$ is formed near the center of the lattice at point b.[30]

[30]This formation of the hexagon with $D = 3$ is due to the uniformity, but this hexagon is

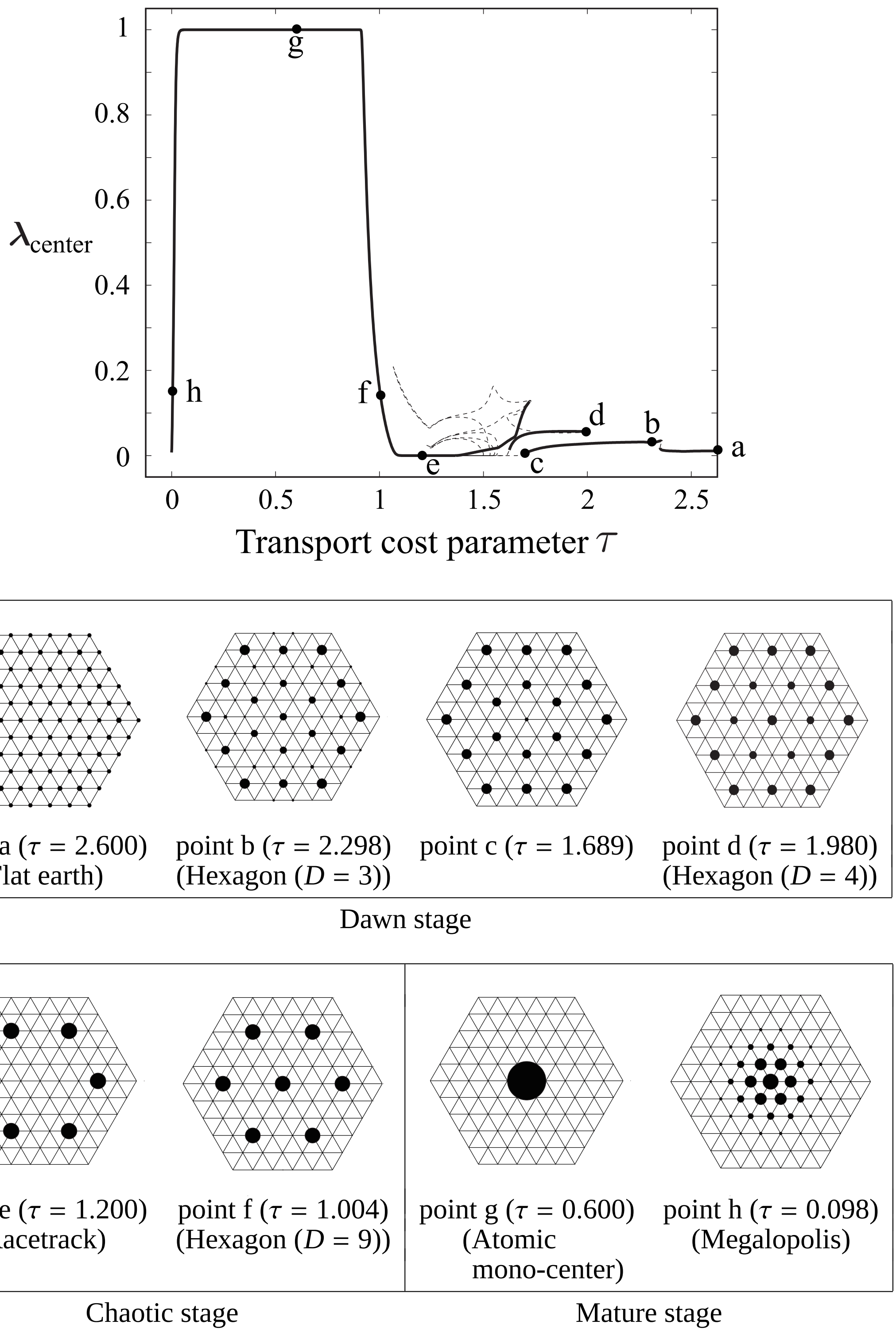

Figure 15: Equilibrium curves and associated population distributions for the standard case with $(\sigma, \mu) = (5.0, 0.4)$.

- In the chaotic stage ($1.1 < \tau < 2.0$), a state of dual stable equilibria of the hexagon with $D = 3$ and that with $D = 4$ (point d) come into existence at $\tau \approx 2$. Thereafter the racetrack (point e) and a hexagon with $D = 9$ (point f) emerge stably. In addition, there are a number of unstable equilibria shown by dashed curves in Fig. 15.

- In the mature stage ($0 < \tau < 1.1$), the atomic mono-center, the megalopolis, and the flat earth occur stably in this order.

As compared in Fig. 16, the durations of stable equilibria for the hexagon with $D = 3$ for the lattices of two kinds shown by the solid and dashed lines display an amazing quantitative agreement. Those of other equilibria exhibit a fair agreement qualitatively. This suffices to show the validity of the "infinite hexagonal lattice analogy" of this paper to extract theoretical information from the lattice without boundary and to describe agglomeration of the lattice with boundary based on this information.

The place at the center of the lattice can be interpreted as the downtown of a city area. The racetrack (point e), which is interpreted as de-centralization leading to downtown decay, is observed as a characteristic economic agglomeration that was overlooked by central place theory but is predicted in the present study. Figure 15 shows recurrences of de-centralization (points c and e) and centralization (point f), i.e., downtown decay and revitalization.

6.2. *Parameter dependence*

Agglomeration is known to be parameter dependent.[31] Parameter dependence of agglomeration is investigated for two parameters: (1) the elasticity σ of substitution between any two varieties and (2) the expenditure share μ of manufactured goods. The formula (33) predicts that agglomeration is accelerated by a lower σ and a higher μ.

6.2.1. *Progress of stable equilibria*

The progress of stable equilibria has been investigated for $\mu = 0.4$ and for various values of the parameter σ ($= 3, 4, 5, 6, 8, 10$), and can be classified as detailed below (see Section 6.1 and Appendix D for examples of these behaviors):

---

blurred away from the center by the spatial asymmetry (inhomogeneity) due to the boundary (see Footnote 5).

[31] For example, Berliant and Yu (2014) [5] demonstrated the dependence of agglomeration on the cost of living.

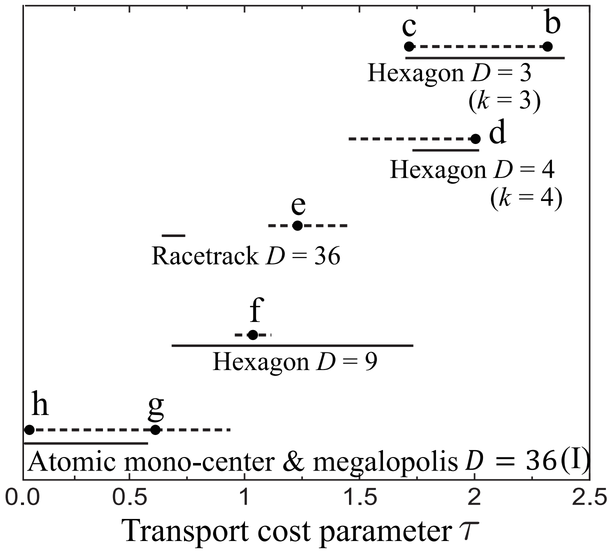

Figure 16: Comparison of progress of stable equilibria for the lattice with boundary (dashed lines) with associated stable equilibria for the lattice without boundary (solid lines).

- Strong agglomeration ($3 \leq \sigma \leq 4$): hexagons with $D = 3$, 4, 9 and 12 emerge stably and agglomeration progresses as

$$\text{Flat earth} \Rightarrow \text{Hexagon } (D = 3) \Rightarrow \text{Hexagon } (D = 4) \Rightarrow$$
$$\left\{ \begin{array}{l} \text{Hexagon } (D = 12) \\ \text{Racetrack} \\ \text{Triangle} \end{array} \right\} \Rightarrow \left\{ \begin{array}{l} \text{Hexagon } (D = 9) \\ \text{Triangle} \end{array} \right\} \Rightarrow$$
$$\text{Atomic mono-center} \Rightarrow \text{Megalopolis} \Rightarrow \text{Flat earth.}$$

- Intermediate agglomeration ($5 \leq \sigma \leq 8$): hexagons with $D = 3$, 4, and 9 emerge stably and agglomeration progresses as

$$\text{Flat earth} \Rightarrow \text{Hexagon } (D = 3) \Rightarrow$$
$$\text{Hexagon } (D = 4) \Rightarrow \text{Racetrack} \Rightarrow \text{Hexagon } (D = 9) \Rightarrow$$
$$\text{Atomic mono-center} \Rightarrow \text{Megalopolis} \Rightarrow \text{Flat earth.}$$

- Weak agglomeration ($\sigma = 10$): no hexagons emerge and agglomeration progresses as

$$\text{Flat earth} \Rightarrow \text{Racetrack} \Rightarrow \text{Triangle} \Rightarrow \text{Racetrack} \Rightarrow$$
$$\text{Atomic mono-center} \Rightarrow \text{Megalopolis} \Rightarrow \text{Flat earth.}$$

In all cases, the agglomeration starts from the flat earth equilibrium and ends up with formation of an atomic mono-center, en route to a megalopolis and the flat earth equilibrium. A racetrack pattern emerges in almost all cases and often transforms into a triangle pattern.[32] More hexagons emerge for a larger agglomeration force.

The influence of parameter μ is investigated for $\sigma = 5.0$ and for $\mu = 0.1$, 0.2, 0.4, 0.5, 0.6, 0.8. These agglomeration can be classified similarly as: strong agglomeration ($0.5 \le \mu \le 0.8$), intermediate agglomeration ($0.2 \le \mu \le 0.4$), and weak agglomeration ($\mu = 0.1$).

6.2.2. Break points

In the investigation of agglomeration under reduced transport costs, it is of economic interest to observe the *break point*, which is defined as the value of τ at the beginning of an increase of downtown population. When investment in transportation infrastructure is committed continuously to enhance downtown population, the break point indexes the functioning of this investment. For the lattice without boundary, this value is given by $\tau_+^{(3)}$ of the hexagon with $D = 3$ for the first bifurcation breaking uniformity (Proposition 5(ii) in Section 4.2).

Figures 17(a) and (b) depict the dependence of break point $\tau_+^{(3)}$ on the values of parameters σ and μ, respectively. As σ increases, the economic balance shifts in favor of dispersion and $\tau_+^{(3)}$ decreases. As μ increases, the economic balance shifts in favor of agglomeration and $\tau_+^{(3)}$ increases.

The break points for the present analysis shown by ($\bullet$) are in good agreement with those for the lattice without boundary shown by (+). In addition, these break points are in agreement with the dashed curve of the theoretical law in (31) and in fair agreement with the approximate law in (33). Such agreement ensures the validity of the basic strategy employed in this paper to extract theoretical information from the lattice without boundary and interpret and describe agglomeration characteristics of the lattice with boundary based on this information.

As made clear in Proposition 2 in Section 4.1, the existence of the break point is conditional on the values of parameters. For $\sigma = 5.0$ and $\theta = 1000$ in Fig. 17(b), the formula (30) gives a condition $\mu > 0.141$ for the existence of break point. Although this condition is violated only for exceptional cases, due regard is paid to the existence of such cases, in which investment in transportation is wasted without leading to economic agglomeration.

[32]This transformation was found in the racetrack economy (Ikeda, Akamatsu, and Kono, 2012a [18]; and Akamatsu, Takayama, and Ikeda, 2012 [1]).

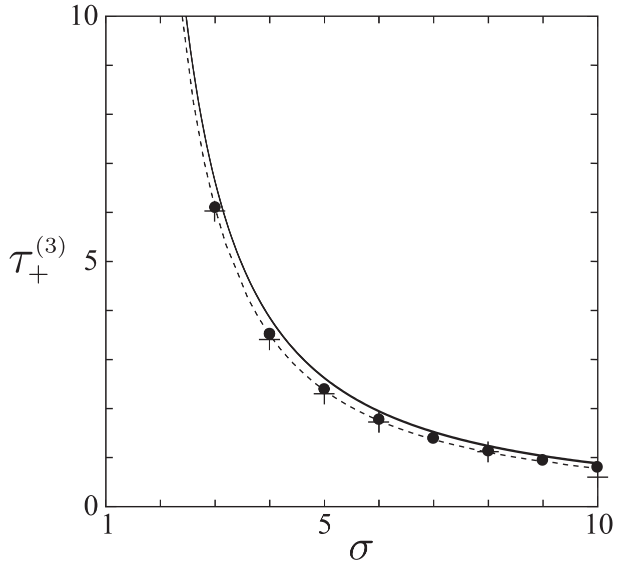

(a) Dependence on σ (μ = 0.4)

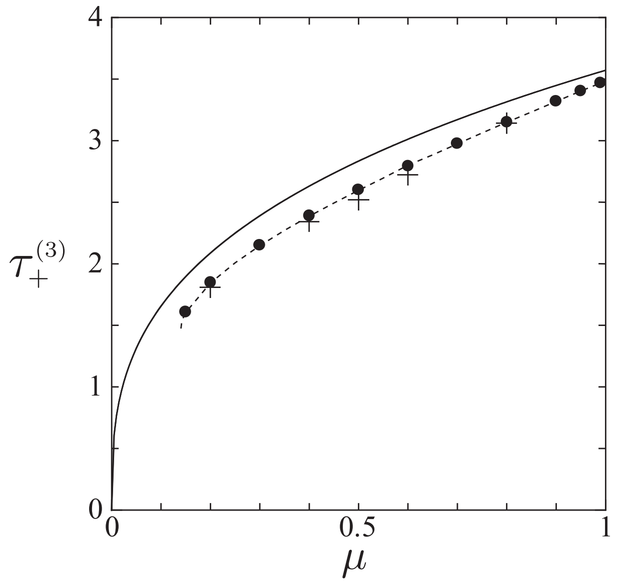

(b) Dependence on μ (σ = 5.0)

Figure 17: Dependence of break point $\tau_+^{(3)}$ on the values of parameters σ and μ (θ = 1000). ($\bullet$) denotes the break point for the present numerical analysis for the lattice with boundary, (+) denotes that for the lattice without boundary, the dashed curve means that for the theoretical law in (31), and the solid curve means that for the approximate law in (33).

7. Conclusion

In this paper, to elucidate the nature of the spatial economic agglomeration, we employed a basic strategy to distinguish spatial properties and microeconomic properties. The former properties are model independent, whereas the latter properties are not.

By the study of spatial properties of a hexagonal lattice without boundary, possible agglomeration patterns on this lattice are found to be hexagons *a la* Christaller and Lösch, racetrack patterns, long narrow patterns, and so on. In particular, racetracks are advanced as a source of de-centralization leading to downtown decay. Agglomeration patterns other than hexagons have not been obtained by the geometrical consideration in central place theory, which demonstrates the usefulness of the theoretical prediction in this paper that goes beyond the scope of central place theory. It is to be emphasized that this theoretical prediction is model independent and applicable to economic models of various kinds.

The stability of equilibria is dependent on microeconomic properties. In order to deepen discussion on the stability, we refered to a specific economic geography model. When the transport cost is reduced from a large value, it was proved that the smallest hexagon is the first non-uniform agglomeration pattern that breaks uniformity. Although this proof was carried out for this specific model, it is extendable to a family of spatial economy models, for which the spatial interaction between places is distant decaying.

There may be a widespread pessimism that stable equilibria in two dimensions are literally infinite and, therefore, cannot be exhausted. Nonetheless, stable equilibria are endowed with geometrically rational forms with rich economic implications and the variety of these forms is quite limited. To rebuff this pessimism, stable equilibria for a specific NEG model were traced under reduced transport costs. Hexagons associated with central place formation have turned out to be most stable and, in turn, to demonstrate the insight of central place theory. Atomic mono-center and megalopolis are stable for small transport costs, whereas racetrack patterns representing de-centralization are sometimes stable. Other patterns are mostly unstable.

An amazing resemblance was observed for the progress of stable agglomerations for the lattice with boundary and that without boundary. This shows the validity and usefulness of the basic strategy employed in this paper to extract theoretical information from the lattice without boundary and interpret and describe agglomeration characteristics of the lattice with boundary based on this information.

If only hexagons were considered in favor of central place theory, possible progress of stable equilibria would be an optimistic one: a continuous increase of the size of hexagons (Fig. 10), leading to continuous growth of the downtown. This, however, is not a true scenario and there is a competition between centralization by hexagons and de-centralization by racetrack patterns. The downtown would recurrently undergo a setback during a short period of the racetrack pattern. In downtown development by investment in transportation, a possible course implied by this study is a bumpy one undergoing several short periods of downtown decay (stable racetrack pattern). Nonetheless, one should not be too pessimistic about such decay as it is just transient and the downtown is destined to be revitalized, en route to development of a megalopolis, if a continuous investment is maintained.

The search for stable economic equilibria in two dimensions is a difficult task. In this paper, such a search was conducted using a core–periphery model that admittedly employs bold assumptions about microeconomy. A future task will be to search for stable equilibria for microeconomic models of various kinds. Nonetheless, the methodology presented in this paper is general and is applicable to other models. For example, possible bifurcating equilibria presented herein would exist universally in the models and, hence, the knowledge of these equilibria would be most useful in search of stable economic equilibria.

References

[1] T. Akamatsu, Y. Takayama, K. Ikeda, Spatial discounting, Fourier, and racetrack economy: A recipe for the analysis of spatial agglomeration models, *Journal of Economic Dynamics and Control* 36(11) (2012) 1729–1759.

[2] A. Anas, Vanishing cities: what does the new economic geography imply about the efficiency of urbanization?, *Journal of Economic Geography* 4(2) (20049 181–199.

[3] S. P. Anderson, A. de Palma, J.-F. Thisse, *Discrete Choice Theory of Product Differentiation*, MIT Press, Cambridge, 1992.

[4] M. J. Beckmann, Spatial equilibrium and the dispersed city, in: Y. Y. Papageorgiou (Ed.), *Mathematical Land Use Theory*, Lexington Books, Lexington, 1976, 117–125.

[5] M. Berliant and C.–M. Yu, Locational signaling and agglomeration MPRA Paper, 55410, Munich 2014.

[6] W. Christaller, *Die zentralen Orte in Süddeutschland*. Gustav Fischer, Jena, 1933. English translation: *Central Places in Southern Germany*. Prentice Hall, Englewood Cliffs, 1966.

[7] M. Clarke, A. G. Wilson, The dynamics of urban spatial structure: The progress of a research programme, *Transactions of the Institute of British Geographers, New Series* 10(4) (1985) 427–451.

[8] P. Dicken, P. E. Lloyd, *Location in Space: Theoretical Perspectives in Economic Geography*, 3rd ed., Harper Collins, New York, 1990.

[9] B. C. Eaton, R. G. Lipsey, The principle of minimum differentiation reconsidered: some new developments in the theory of spatial competition, *The Review of Economic Studies* 42(1) (1975) 27–49.

[10] B. C. Eaton, R. G. Lipsey, An economic theory of central places, *The Economic Journal* 92(365) (1982) 56–72.

[11] H. Flam, E. Helpman, Industrial policy under monopolistic competition, *Journal of International Economics* 22 (1987) 79-102.

[12] R. Forslid, G. I. P. Ottaviano, An analytically solvable core-periphery model, *Journal of Economic Geography* 3 (2003) 229–340.

[13] D. Fudenberg, D. K. Levine, *The Theory of Learning in Games*, MIT Press, Cambridge, 1998.

[14] M. Fujita, P. Krugman, T. Mori, On the evolution of hierarchical urban systems, *European Economic Review* 43(2) (1999a) 209–251.

[15] M. Fujita, P. Krugman, A. J. Venables, *The Spatial Economy: Cities, Regions, and International Trade*, MIT Press, Cambridge, 1999b.

[16] M. Fujita, T. Mori, Structural stability and the evolution of urban systems, *Regional Science and Urban Economics* 42 (1997) 399–442.

[17] M. Fujita, H. Ogawa, Multiple equilibria and structural transition of non-monocentric urban configurations, *Regional Science and Urban Economics* 12(2) (1982) 161–196.

[18] K. Ikeda, T. Akamatsu, T. Kono, Spatial period-doubling agglomeration of a core–periphery model with a system of cities, *Journal of Economic Dynamics and Control* 36 (2012a) 754–778.

[19] K. Ikeda, K. Murota, *Imperfect Bifurcation in Structures and Materials*, 2nd ed., Springer-Verlag, New York, 2010.

[20] K. Ikeda, K. Murota, *Bifurcation Theory for Hexagonal Agglomeration in Economic Geography*, Springer-Verlag, Tokyo, 2014.

[21] K. Ikeda, K. Murota, T. Akamatsu, Self-organization of Lösch's hexagons in economic agglomeration for core–periphery models. *International Journal of Bifurcation and Chaos* 22(8) (2012b) 1230026-1–1230026-29.

[22] K. Ikeda, K. Murota, T. Akamatsu, T. Kono, Y. Takayama, Self-organization of hexagonal agglomeration patterns in new economic geography models, *Journal of Economic Behavior & Organization* 99 (2014) 32–52.

[23] P. Krugman, Increasing returns and economic geography, *Journal of Political Economy* 99 (1991) 483–499.

[24] P. Krugman, On the number and location of cities, *European Economic Review* 37 (1993) 293–298.

[25] A. Lösch, *Die räumliche Ordnung der Wirtschaft*. Gustav Fischer, Jena, 1940. English translation: *The Economics of Location*. Yale University Press, New Haven, 1954.

[26] T. Mori, A modeling of megalopolis formation: the maturing of city systems, *Journal of Urban Economics* 42 (1997) 133–157.

[27] P. Mossay, P. M. Picard, On spatial equilibria in a social interaction model, *Journal of Economic Theory* 146(6) (2011) 2455–2477.

[28] M. Munz, W. Weidlich, Settlement formation, Part II: Numerical simulation, *The Annals of Regional Science* 24 (1990) 177–196.

[29] Y. Murata, Product diversity, taste heterogeneity, and geographic distribution of economic activities: market vs. non-market interactions, *Journal of Urban Economics* 53(1) (2003) 126–144.

[30] G. Ottaviano, T. Tabuchi, J.-F. Thisse, Agglomeration and trade revisited, *International Economic Review* 43(2) (2002) 409–435.

[31] D. Oyama, Agglomeration under forward-looking expectations: Potentials and global stability, *Regional Science and Urban Economics* 39(6) (2009) 696–713.

[32] P. M. Picard, T. Tabuchi, Self-organized agglomerations and transport costs, *Economic Theory* 42 (2010) 565–589.

[33] D. Stelder, Where do cities form? A geographical agglomeration model for Europe, *Journal of Regional Science* 45 (2005) 657–679.

[34] T. Tabuchi, Urban agglomeration economies in a linear city, *Regional Science and Urban Economics* 16(3) (1986) 421–436.

[35] T. Tabuchi, J.-F. Thisse, Taste heterogeneity, labor mobility and economic geography, *Journal of Development Economics* 69 (2002) 155–177.

[36] T. Tabuchi, J.-F. Thisse, A new economic geography model of central places, *Journal of Urban Economics* 69 (2011) 240–252.

Appendix A. Theoretical details

Several theoretical details are contained in this appendix.

Appendix A.1. Eigenvectors of the Jacobian matrix

Eigenvectors of the Jacobian matrix J of the governing equation (3) for the 6×6 hexagonal lattice are presented as a summary of Ikeda and Murota (2014) [20]. To begin with, we define a matrix

$$Q = (Q^{(1)}, Q^{(3)}, Q^{(4)}, Q^{(9)}, Q^{(12)}, Q^{(36(\mathrm{I}))}, Q^{(36(\mathrm{II}))}),$$

where

$$Q^{(k)} = (\boldsymbol{q}_1^{(k)}, \boldsymbol{q}_2^{(k)}, \ldots), \quad k = 1, 3, 4, 9, 12, 36(\mathrm{I}), 36(\mathrm{II}). \tag{A.1}$$

The matrix $Q^{(k)}$ in this equation consists of the eigenvectors $\boldsymbol{q}_1^{(k)}, \boldsymbol{q}_2^{(k)}, \ldots$ given in this appendix (cf., Remark 1).

The coordinate of a place on the $n \times n$ hexagonal lattice is given by

$$\boldsymbol{x} = n_1\boldsymbol{\ell}_1 + n_2\boldsymbol{\ell}_2, \quad n_1, n_2 = 0, 1, \ldots, n-1$$

with $n = 6$ for the present case, $\boldsymbol{\ell}_1 = l(1, 0)^\top$, and $\boldsymbol{\ell}_2 = l(-1/2, \sqrt{3}/2)^\top$. Thus, the $K = n^2$ places are indexed by (n_1, n_2). The vector $\boldsymbol{\lambda}$ expressing population distribution is defined as

$$\begin{aligned} \boldsymbol{\lambda} &= (\lambda_1, \ldots, \lambda_K)^\top \\ &= (\lambda_{00}, \ldots, \lambda_{n-1,0};\ \lambda_{01}, \ldots, \lambda_{n-1,1};\ \ldots\ ;\ \lambda_{0,n-1}, \ldots, \lambda_{n-1,n-1})^\top \\ &= (\lambda_{n_1 n_2} \mid n_1, n_2 = 0, \ldots, n-1), \end{aligned}$$

where $(\lambda_{n_1 n_2} \mid n_1, n_2 = 0, \ldots, n-1)$ is a K-dimensional column vector. A vector on this lattice with the (n_1, n_2)-component $g(n_1, n_2)$ is normalized as

$$\langle g(n_1, n_2)\rangle = (g(n_1, n_2)/(\sum_{i=0}^{n-1}\sum_{j=0}^{n-1} g(i, j)^2)^{1/2} \mid n_1, n_2 = 0, \ldots, n-1). \tag{A.2}$$

Then a concrete form of each $Q^{(k)}$ in (A.1) is given below.

$$
\begin{aligned}
Q^{(1)} &= \frac{1}{6}(1, \ldots, 1)^\top, && \text{(A.3)}\\
Q^{(3)} &= [\boldsymbol{q}_1^{(3)}, \boldsymbol{q}_2^{(3)}] \\
&= [\langle \cos(2\pi(n_1 - 2n_2)/3)\rangle, \langle \sin(2\pi(n_1 - 2n_2)/3)\rangle], && \text{(A.4)}\\
Q^{(4)} &= [\boldsymbol{q}_1^{(4)}, \boldsymbol{q}_2^{(4)}, \boldsymbol{q}_3^{(4)}] \\
&= [\langle \cos(\pi n_1)\rangle, \langle \cos(\pi n_2)\rangle, \langle \cos(\pi(n_1 - n_2))\rangle], && \text{(A.5)}\\
Q^{(9)} &= [\boldsymbol{q}_1^{(9)}, \ldots, \boldsymbol{q}_6^{(9)}] \\
&= [\ \langle \cos(2\pi\, n_1/3)\rangle,\ \langle \sin(2\pi\, n_1/3)\rangle, \\
&\quad \langle \cos(2\pi(-n_2)/3)\rangle,\ \langle \sin(2\pi(-n_2)/3)\rangle, \\
&\quad \langle \cos(2\pi(-n_1 + n_2)/3)\rangle,\ \langle \sin(2\pi(-n_1 + n_2)/3)\rangle], && \text{(A.6)}\\
Q^{(12)} &= [\boldsymbol{q}_1^{(12)}, \ldots, \boldsymbol{q}_6^{(12)}] \\
&= [\ \langle \cos(\pi(n_1 + n_2)/3)\rangle,\ \langle \sin(\pi(n_1 + n_2)/3)\rangle, \\
&\quad \langle \cos(\pi(n_1 - 2n_2)/3)\rangle,\ \langle \sin(\pi(n_1 - 2n_2)/3)\rangle, \\
&\quad \langle \cos(\pi(-2n_1 + n_2)/3)\rangle,\ \langle \sin(\pi(-2n_1 + n_2)/3)\rangle\ ], && \text{(A.7)}\\
Q^{(36(\mathrm{I}))} &= [\boldsymbol{q}_1^{(36(\mathrm{I}))}, \ldots, \boldsymbol{q}_6^{(36(\mathrm{I}))}] \\
&= [\ \langle \cos(\pi\, n_1/3)\rangle,\ \langle \sin(\pi\, n_1/3)\rangle, \\
&\quad \langle \cos(\pi(-n_2)/3)\rangle,\ \langle \sin(\pi(-n_2)/3)\rangle, \\
&\quad \langle \cos(\pi(-n_1 + n_2)/3)\rangle,\ \langle \sin(\pi(-n_1 + n_2)/3)\rangle], && \text{(A.8)}\\
Q^{(36(\mathrm{II}))} &= [\boldsymbol{q}_1^{(36(\mathrm{II}))}, \ldots, \boldsymbol{q}_{12}^{(36(\mathrm{II}))}] \\
&= [\ \langle \cos(2\pi(2n_1 + n_2)/n)\rangle,\ \langle \sin(2\pi(2n_1 + n_2)/n)\rangle, \\
&\quad \langle \cos(2\pi(n_1 - 3n_2)/n)\rangle,\ \langle \sin(2\pi(n_1 - 3n_2)/n)\rangle, \\
&\quad \langle \cos(2\pi(-3n_1 + 2n_2)/n)\rangle,\ \langle \sin(2\pi(-3n_1 + 2n_2)/n)\rangle, \\
&\quad \langle \cos(2\pi(2n_1 - 3n_2)/n)\rangle,\ \langle \sin(2\pi(2n_1 - 3n_2)/n)\rangle, \\
&\quad \langle \cos(2\pi(n_1 + 2n_2)/n)\rangle,\ \langle \sin(2\pi(n_1 + 2n_2)/n)\rangle, \\
&\quad \langle \cos(2\pi(-3n_1 + 2n_2)/n)\rangle,\ \langle \sin(2\pi(-3n_1 + 2n_2)/n)\rangle]. && \text{(A.9)}
\end{aligned}
$$

By the so called group-theoretic analysis, the eigenvectors for Lösch's hexagons are obtained as

$$\begin{aligned}
\boldsymbol{q}^{(3)} &= \boldsymbol{q}_1^{(3)} = \langle\cos(2\pi(n_1 - 2n_2)/3)\rangle, && \text{(A.10)}\\
\boldsymbol{q}^{(4)} &= \boldsymbol{q}_1^{(4)} + \boldsymbol{q}_2^{(4)} + \boldsymbol{q}_3^{(4)}\\
&= \langle\cos(\pi n_1)\rangle + \langle\cos(\pi n_2)\rangle + \langle\cos(\pi(n_1 - n_2))\rangle, && \text{(A.11)}\\
\boldsymbol{q}^{(9)} &= \boldsymbol{q}_1^{(9)} + \boldsymbol{q}_3^{(9)} + \boldsymbol{q}_5^{(9)}\\
&= \langle\cos(2\pi\, n_1/3)\rangle + \langle\cos(2\pi(-n_2)/3)\rangle + \langle\cos(2\pi(-n_1 + n_2)/3)\rangle, && \text{(A.12)}\\
\boldsymbol{q}^{(12)} &= \boldsymbol{q}_1^{(12)} + \boldsymbol{q}_3^{(12)} + \boldsymbol{q}_5^{(12)}\\
&= \cos(\pi(n_1 + n_2)/3)\rangle + \cos(\pi(n_1 - 2n_2)/3)\rangle + \langle\cos(\pi(-2n_1 + n_2)/3)\rangle,\\
& && \text{(A.13)}\\
\boldsymbol{q}^{(36(\mathrm{I}))} &= \boldsymbol{q}_1^{(36(\mathrm{I}))} + \boldsymbol{q}_3^{(36(\mathrm{I}))} + \boldsymbol{q}_5^{(36(\mathrm{I}))}\\
&= \langle\cos(\pi\, n_1/3)\rangle + \langle\cos(\pi(-n_2)/3)\rangle + \langle\cos(\pi(-n_1 + n_2)/3)\rangle, && \text{(A.14)}\\
\boldsymbol{q}^{(36(\mathrm{II}))} &= \boldsymbol{q}_1^{(36(\mathrm{II}))} + \boldsymbol{q}_3^{(36(\mathrm{II}))} + \boldsymbol{q}_5^{(36(\mathrm{II}))} + \boldsymbol{q}_7^{(36(\mathrm{II}))} + \boldsymbol{q}_9^{(36(\mathrm{II}))} + \boldsymbol{q}_{11}^{(36(\mathrm{II}))}\\
&= \langle\cos(2\pi(2n_1 + n_2)/n)\rangle + \langle\cos(2\pi(n_1 - 3n_2)/n)\rangle\\
&\quad + \langle\cos(2\pi(-3n_1 + 2n_2)/n)\rangle + \langle\cos(2\pi(2n_1 - 3n_2)/n)\rangle\\
&\quad + \langle\cos(2\pi(n_1 + 2n_2)/n)\rangle + \langle\cos(2\pi(-3n_1 + 2n_2)/n)\rangle. && \text{(A.15)}
\end{aligned}$$

Remark 1. In consulting Ikeda and Murota (2014) [20], note the correspondence:

$$\begin{aligned}
&1, 3, 4, 9, 12, 36(\mathrm{I}), 36(\mathrm{II})\\
\Longleftrightarrow\quad &(1; +, +), (2; +), (3; +, +), (6; 2, 0, +), (6; 1, 1, +), (6; 1, 0, +), (12; 2, 1)
\end{aligned}$$

between the notations in the present study and Ikeda and Murota (2014) [20]. □

Appendix A.2. Group-theoretic analysis of a bifurcation point of multiplicity 12

A bifurcating solution for the deformed hexagon is obtained. Let us consider the equilibrium equation

$$\boldsymbol{F}(\boldsymbol{\lambda}, \tau) = \boldsymbol{0} \tag{A.16}$$

for the 6×6 hexagonal lattice without boundary. This equation has the pre-bifurcation flat earth equilibria $\boldsymbol{\lambda} = \frac{1}{6^2}(1, \ldots, 1)^\top$.

Let $(\boldsymbol{\lambda}_c, \tau_c)$ be a critical point of multiplicity 12 on the flat earth equilibria. This point is related to the eigenvectors $\boldsymbol{q}_1^{(36(\mathrm{II}))}, \ldots, \boldsymbol{q}_{12}^{(36(\mathrm{II}))}$ in (6) with $k = 36(\mathrm{II})$. By Liapunov–Schmidt reduction, the full system of equilibrium equation (A.16) is reduced, in a neighborhood of the critical point $(\boldsymbol{\lambda}_c, \tau_c)$, to a system of bifurcation equations

$$\widetilde{\boldsymbol{F}}(\boldsymbol{w}, \widetilde{\tau}) = \boldsymbol{0} \tag{A.17}$$

in $\boldsymbol{w} = (w_1, \ldots, w_{12})^\top$, where $\boldsymbol{w}$ is defined by $\boldsymbol{\lambda} = \boldsymbol{\lambda}_{\mathrm{c}} + \sum_{i=1}^{12} w_i \boldsymbol{q}_i^{(36(\mathrm{II}))}$, $\widetilde{\boldsymbol{F}}$ is a 12-dimensional vector of functions, and $\widetilde{\tau} = \tau - \tau_{\mathrm{c}}$ denotes the increment of τ. In this reduction process the symmetry of the full system is inherited by the reduced system (A.17). Moreover, the existence of bifurcating solutions can be determined by analysis of the reduced system as each $\boldsymbol{w}$ uniquely determines a solution $\boldsymbol{\lambda}$ to the full system (A.16).

The bifurcation equation (A.17) for the critical point of multiplicity 12 is a 12-dimensional equation over $\mathbb{R}$. This equation can be expressed as a 6-dimensional complex-valued equation in complex variables $z_j = w_{2j-1} + \mathrm{i} w_{2j}$ $(j = 1, \ldots, 6)$ as

$$F_i(z_1, \ldots, z_6, \bar{z}_1, \ldots, \bar{z}_6, \widetilde{\tau}) = 0, \quad i = 1, \ldots, 6, \tag{A.18}$$

where

$$(z_1, \ldots, z_6, \bar{z}_1, \ldots, \bar{z}_6, \widetilde{\tau}) = (0, \ldots, 0, 0, \ldots, 0, 0)$$

is assumed to correspond to the critical point. For notational simplicity we write (A.18) as

$$F_i(z_1, \ldots, z_6) = 0, \quad i = 1, \ldots, 6 \tag{A.19}$$

by omitting $\bar{z}_1, \ldots, \bar{z}_6$ and $\widetilde{\tau}$ in the subsequent derivation.

We expand F_1 as

$$\begin{aligned} &F_1(z_1, z_2, z_3, z_4, z_5, z_6) \\ &= \sum_{a=0} \sum_{b=0} \cdots \sum_{u=0} A_{abcdeghijstu}(\widetilde{\tau}) z_1^a z_2^b z_3^c z_4^d z_5^e z_6^g \bar{z}_1^h \bar{z}_2^i \bar{z}_3^j \bar{z}_4^s \bar{z}_5^t \bar{z}_6^u. \end{aligned} \tag{A.20}$$

Since $(z_1, z_2, z_3, z_4, z_5, z_6, \widetilde{\tau}) = (0, 0, 0, 0, 0, 0, 0)$ corresponds to the critical point of multiplicity 12, we have

$$A_{000000000000}(0) = 0, \tag{A.21}$$

$$A_{100000000000}(0) = A_{010000000000}(0) = \cdots = A_{000000000001}(0) = 0. \tag{A.22}$$

By virtue of the symmetry of the lattice, $F_2, \ldots, F_6$ are obtained from F_1 as

$$F_2(z_1, z_2, z_3, z_4, z_5, z_6) = F_1(z_2, z_3, z_1, z_6, z_4, z_5), \tag{A.23}$$

$$F_3(z_1, z_2, z_3, z_4, z_5, z_6) = F_1(z_3, z_1, z_2, z_5, z_6, z_4), \tag{A.24}$$

$$F_4(z_1, z_2, z_3, z_4, z_5, z_6) = F_1(z_4, z_5, z_6, z_1, z_2, z_3), \tag{A.25}$$

$$F_5(z_1, z_2, z_3, z_4, z_5, z_6) = F_1(z_5, z_6, z_4, z_3, z_1, z_2), \tag{A.26}$$

$$F_6(z_1, z_2, z_3, z_4, z_5, z_6) = F_1(z_6, z_4, z_5, z_2, z_3, z_1), \tag{A.27}$$

the coefficients $A_{abcdeghijstu}(\widetilde{\tau})$ in (A.20) are real, and the indices $(a, b, \ldots, t, u)$ of nonvanishing coefficients $A_{ab\cdots tu}(\widetilde{\tau})$ in (A.20) must satisfy[33]

$$2(a-h)+(b-i)-3(c-j)+2(d-s)+(e-t)-3(g-u) \equiv 2 \mod 6, \tag{A.28}$$

$$(a-h)-3(b-i)+2(c-j)-3(d-s)+2(e-t)+(g-u) \equiv 1 \mod 6. \tag{A.29}$$

We denote by S the set of nonnegative indices $(a, b, \ldots, t, u)$ that satisfy the above conditions, i.e.,

$$S = \{(a, b, \ldots, t, u) \in \mathbb{Z}_+^{12} \mid \text{(A.28) and (A.29)}\}, \tag{A.30}$$

where $\mathbb{Z}_+$ represents the set of nonnegative integers. Then $(a, b, \ldots, t, u)$ must belong to S if $A_{ab\cdots tu}(\widetilde{\tau}) \neq 0$, and hence (A.20) can be replaced by

$$F_1(z_1, z_2, z_3, z_4, z_5, z_6) = \sum_S A_{abcdeghijstu}(\widetilde{\tau}) z_1^a z_2^b z_3^c z_4^d z_5^e z_6^g \bar{z}_1^h \bar{z}_2^i \bar{z}_3^j \bar{z}_4^s \bar{z}_5^t \bar{z}_6^u. \tag{A.31}$$

We have $A_{ab\cdots tu}(\widetilde{\tau}) \neq 0$ (generically) for $(a, b, \ldots, t, u) \in S$. The expanded form (A.31), for $n = 6$, takes a special form

$$\begin{aligned} F_1 \;\; = \;\; & A_1 z_1 + A_2 \bar{z}_2 \bar{z}_3 + (A_3 z_1^2 \bar{z}_1 + A_4 z_1 z_2 \bar{z}_2 + A_5 z_1 z_3 \bar{z}_3 + A_6 z_1 z_4 \bar{z}_4 + A_7 z_1 z_5 \bar{z}_5 \\ & + A_8 z_1 z_6 \bar{z}_6 + A_9 z_2 \bar{z}_4 z_6 + A_{10} z_3 \bar{z}_4 z_5 + A_{11} \bar{z}_1 z_2 \bar{z}_6 + A_{12} z_3^2 z_4 + A_{13} \bar{z}_1 \bar{z}_5^2) \\ & + [A_{14} z_4 \bar{z}_6^2 + A_{15} \bar{z}_5 z_6^3 + A_{16} \bar{z}_5 \bar{z}_6^3 + \cdots] + \cdots \end{aligned} \tag{A.32}$$

for some constants A_i ($i = 1, 2, \ldots$); see Example 9.1 of Ikeda and Murota (2014) [20].

We search for bifurcating solutions of the forms

$$z_1 = x, \quad z_2 = z_3 = z_4 = z_5 = z_6 = 0,$$

with $x \in \mathbb{R}$ and $x \neq 0$. Using (A.23)–(A.27) and (A.31) with (A.28) and (A.29) to

[33] Equations (A.28) and (A.29), respectively, correspond to (9.100) and (9.101) with $(k, \ell, n) = (2, 1, 6)$ in Ikeda and Murota (2014) [20].

(A.30), we obtain a set of equations

$$\begin{aligned}
F_1(x,0,0,0,0,0) &= \sum_S A_{a00000h00000}(\widetilde{\tau})x^{a+h} = \sum_{a-h\equiv 1 \mod 6} A_{a00000h00000}(\widetilde{\tau})x^{a+h}, \\
F_2(x,0,0,0,0,0) &= F_1(0,0,x,0,0,0) = \sum_S A_{00c00000j000}(\widetilde{\tau})x^{c+j} = 0, \\
F_3(x,0,0,0,0,0) &= F_1(0,x,0,0,0,0) = \sum_S A_{0b00000i0000}(\widetilde{\tau})x^{b+i} = 0, \\
F_4(x,0,0,0,0,0) &= F_1(0,0,0,x,0,0) = \sum_S A_{000d00000s00}(\widetilde{\tau})x^{d+s} = 0, \\
F_5(x,0,0,0,0,0) &= F_1(0,0,0,0,x,0) = \sum_S A_{0000e00000t0}(\widetilde{\tau})x^{e+t} = 0, \\
F_6(x,0,0,0,0,0) &= F_1(0,0,0,0,0,x) = \sum_S A_{00000g00000u}(\widetilde{\tau})x^{g+u} = 0.
\end{aligned}$$

Since $a + h \geq 1$ for each (a, h) with $a - h \equiv 1 \mod 6$, it is possible to divide the first equation by x to arrive at

$$\frac{1}{x} F_1(x,0,0,0,0,0) = \sum_{a-h\equiv 1 \mod 6} A_{a00000h00000}(\widetilde{\tau})x^{a+h-1},$$

and the bifurcating solution is determined from

$$\sum_{a-h\equiv 1 \mod 6} A_{a00000h00000}(\widetilde{\tau})x^{a+h-1} = 0. \tag{A.33}$$

The leading terms of (A.33) are given as

$$A\widetilde{\tau} + Bx^2 = 0$$

with generically nonzero coefficients $A = A'_{100000000000}(0)$ and $B = A_{200000100000}(0)$, where $(\ )'$ denotes the derivative with respect to τ. By the implicit function theorem, the equation (A.33) can be solved for x as

$$x = \psi_{\mathrm{II}}(\widetilde{\tau}),$$

where

$$\psi_{\mathrm{II}}(\widetilde{\tau}) \approx \pm\sqrt{-\frac{A}{B}\widetilde{\tau}}, \quad \widetilde{\tau} \to 0$$

with $-A/B \neq 0$. Hence, we obtain a bifurcating solution

$$z_1 = \psi_{\mathrm{II}}(\widetilde{\tau}), \quad z_2 = z_3 = z_4 = z_5 = z_6 = 0.$$

This equation indicates the existence of a bifurcating solution in the direction of $(w_1, \ldots, w_{12}) = (1, 0, \ldots, 0)$, i.e., $\boldsymbol{q}_1^{(36(\mathrm{II}))}$. This solution corresponds to the deformed hexagon introduced in Fig. 9.

Appendix B. Derivation of formulas for the break point

Formulas for the break point presented in Section 4 are derived. The method in Akamatsu, Takayama, and Ikeda (2012) [1] is adapted to the 6×6 hexagonal lattice without boundary.

Appendix B.1. Eigenanalysis of spatial discounting matrix

Recall the spatial discounting matrix $D = (d_{ij})$ in (10) with

$$d_{ij} = r^{\,m(i,j)} \tag{B.1}$$

and

$$r = \exp[-\tau(\sigma - 1)\tilde{L}] \tag{B.2}$$

in (23). The nominal length $\hat{L}$ of the road is chosen as $\hat{L} = 1/n = 1/6$.

The spatial discounting matrix D for the 6×6 hexagonal lattice takes the form:

$$D = \begin{bmatrix} D_0 & D_1 & D_2 & D_3 & D_4 & D_5 \\ D_5 & D_0 & D_1 & D_2 & D_3 & D_4 \\ D_4 & D_5 & D_0 & D_1 & D_2 & D_3 \\ D_3 & D_4 & D_5 & D_0 & D_1 & D_2 \\ D_2 & D_3 & D_4 & D_5 & D_0 & D_1 \\ D_1 & D_2 & D_3 & D_4 & D_5 & D_0 \end{bmatrix},$$

which is a block-circulant matrix made up of circulant matrices:

$$D_0 = \begin{bmatrix} 1 & r & r^2 & r^3 & r^2 & r \\ r & 1 & r & r^2 & r^3 & r^2 \\ r^2 & r & 1 & r & r^2 & r^3 \\ r^3 & r^2 & r & 1 & r & r^2 \\ r^2 & r^3 & r^2 & r & 1 & r \\ r & r^2 & r^3 & r^2 & r & 1 \end{bmatrix}, \quad D_1 = D_5{}^{\top} = \begin{bmatrix} r & r & r^2 & r^3 & r^3 & r^2 \\ r^2 & r & r & r^2 & r^3 & r^3 \\ r^3 & r^2 & r & r & r^2 & r^3 \\ r^3 & r^3 & r^2 & r & r & r^2 \\ r^2 & r^3 & r^3 & r^2 & r & r \\ r & r^2 & r^3 & r^3 & r^2 & r \end{bmatrix},$$

$$D_2 = D_4{}^{\top} = \begin{bmatrix} r^2 & r^2 & r^2 & r^3 & r^4 & r^3 \\ r^3 & r^2 & r^2 & r^2 & r^3 & r^4 \\ r^4 & r^3 & r^2 & r^2 & r^2 & r^3 \\ r^3 & r^4 & r^3 & r^2 & r^2 & r^2 \\ r^2 & r^3 & r^4 & r^3 & r^2 & r^2 \\ r^2 & r^2 & r^3 & r^4 & r^3 & r^2 \end{bmatrix}, \quad D_3 = r^3 \begin{bmatrix} 1 & 1 & 1 & 1 & 1 & 1 \\ 1 & 1 & 1 & 1 & 1 & 1 \\ 1 & 1 & 1 & 1 & 1 & 1 \\ 1 & 1 & 1 & 1 & 1 & 1 \\ 1 & 1 & 1 & 1 & 1 & 1 \\ 1 & 1 & 1 & 1 & 1 & 1 \end{bmatrix}.$$

The direct bifurcation from the flat earth equilibrium $\boldsymbol{\lambda}^* = \frac{1}{K}(1, \ldots, 1)^\top$ ($K = n^2 = 6^2$) in the direction of the eigenvector

$$\boldsymbol{\eta} = \boldsymbol{q}^{(k)}, \qquad k = 3, 4, 9, 12, 36(\mathrm{I}), 36(\mathrm{II}) \tag{B.3}$$

of $J(\boldsymbol{\lambda}^*)$ is investigated, where $\boldsymbol{q}^{(k)}$ is given in (A.10)–(A.15).

It is easy to verify that the vector $\boldsymbol{\eta}$ is also an eigenvector of the spatial discounting matrix D, i.e.,

$$D\boldsymbol{\eta} = \tilde{\epsilon}^{(k)}\boldsymbol{\eta}, \quad k = 3, 4, 9, 12, 36(\mathrm{I}), 36(\mathrm{II}) \tag{B.4}$$

with

$$\tilde{\epsilon}^{(k)} = \tilde{\epsilon}^{(k)}(r) = \begin{cases} 1 - 3r + 3r^2 - 3r^3 + 2r^4 & \text{for } k = 3, \\ 1 - 2r + 4r^2 - 5r^3 + 2r^4 & \text{for } k = 4, \\ 1 - 3r^2 + 3r^3 - r^4 & \text{for } k = 9, \\ 1 + r - 5r^2 + r^3 + 2r^4 & \text{for } k = 12, \\ 1 + 4r + r^2 - 5r^3 - r^4 & \text{for } k = 36(\mathrm{I}), \\ 1 - 2r + r^2 + r^3 - r^4 & \text{for } k = 36(\mathrm{II}). \end{cases} \tag{B.5}$$

Denote by d the sum of the entries of a column of D, which is given by

$$d = \sum_{i=1}^{K} r^{\,m(i,j)} = 1 + 6r + 12r^2 + 15r^3 + 2r^4. \tag{B.6}$$

Then, for the vector $\boldsymbol{\eta}$ in (B.4), we have

$$\frac{D}{d}\boldsymbol{\eta} = \epsilon\boldsymbol{\eta}$$

with

$$\epsilon = \frac{\tilde{\epsilon}^{(k)}}{d}, \tag{B.7}$$

where (B.4), (B.5) and (B.6) are used. Since $0 < r < 1$, we have

$$\epsilon < 1, \tag{B.8}$$

as shown in Fig. B.1. By the implicit function theorem, (B.7) yields

$$r = \Phi^{(k)}(\epsilon) \tag{B.9}$$

for some function $\Phi^{(k)}$.

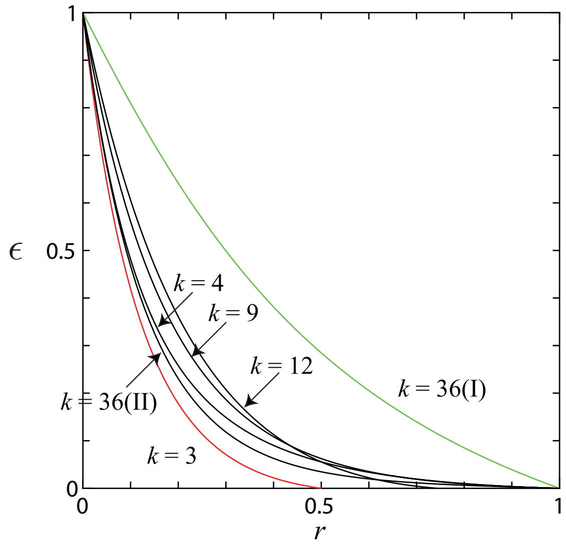

Figure B.1: Curves of ϵ plotted against r $(0 < r < 1)$.

Appendix B.2. Break point for hexagons

From the governing equation $\boldsymbol{F}$ in (27) with $H = 1$, we have

$$\frac{\partial F_i}{\partial \lambda_j} = \sum_{k=1}^{K} \frac{\partial F_i}{\partial v_k}\frac{\partial v_k}{\partial \lambda_j} - \delta_{ij} = -\theta \sum_{k=1}^{K} P_i P_k \frac{\partial v_k}{\partial \lambda_j} + \theta P_i \frac{\partial v_i}{\partial \lambda_j} - \delta_{ij}, \tag{B.10}$$

where δ_{ij} is the Kronecker delta. This shows that the Jacobian matrices

$$J(\lambda) = \frac{\partial \boldsymbol{F}}{\partial \boldsymbol{\lambda}} = \left(\frac{\partial F_i}{\partial \lambda_j}\right), \quad V(\lambda) = \frac{\partial \boldsymbol{v}}{\partial \boldsymbol{\lambda}} = \left(\frac{\partial v_i}{\partial \lambda_j}\right)$$

are related as

$$J(\lambda) = -\theta \begin{bmatrix} P_1 \\ \vdots \\ P_K \end{bmatrix} \begin{bmatrix} P_1 \cdots P_K \end{bmatrix} V(\lambda) + \theta \begin{bmatrix} P_1 & & \\ & \ddots & \\ & & P_K \end{bmatrix} V(\lambda) - I, \tag{B.11}$$

where I is the identity matrix.

In regard to $V(\lambda)$ we recall (25):

$$v_i(\boldsymbol{\lambda}, \tau) = \frac{\mu}{\sigma - 1} \log \Delta_i(\boldsymbol{\lambda}, \tau) + \log[w_i(\boldsymbol{\lambda}, \tau)] \tag{B.12}$$

as well as (24):

$$w_i(\boldsymbol{\lambda}, \tau) = \frac{\mu}{\sigma} \sum_k \frac{d_{ik}}{\Delta_k(\boldsymbol{\lambda}, \tau)} (w_k(\boldsymbol{\lambda}, \tau)\lambda_k + 1), \tag{B.13}$$

where

$$\Delta_k(\boldsymbol{\lambda}, \tau) = \Delta_k = \sum_{j=1}^{K} d_{jk}\lambda_j.$$

The differentiations of (B.12) and (B.13) with respect to λ_j yield, respectively,

$$\begin{aligned}\frac{\partial v_i}{\partial \lambda_j} &= \kappa' \frac{d_{ji}}{\Delta_i} + \frac{1}{w_i}\frac{\partial w_i}{\partial \lambda_j}, &\text{(B.14)}\\ \frac{\partial w_i}{\partial \lambda_j} &= \kappa \sum_{k=1}^{K} \frac{d_{ik}}{{\Delta_k}^2}\left[\left(\frac{\partial w_k}{\partial \lambda_j}\lambda_k + w_k\delta_{kj}\right)\Delta_k - (w_k\lambda_k + 1)d_{jk}\right], &\text{(B.15)}\end{aligned}$$

where

$$\kappa = \frac{\mu}{\sigma}, \quad \kappa' = \frac{\mu}{\sigma - 1}. \tag{B.16}$$

We have $0 < \kappa < 1$ and $\kappa' > 0$ because $\sigma > 1$, $0 < \mu < 1$.

At the flat earth equilibrium $\boldsymbol{\lambda}^* = \frac{1}{K}(1, \ldots, 1)^\top$, (B.11) yields

$$J(\boldsymbol{\lambda}^*) = -\frac{\theta}{K^2}\mathbf{1}\mathbf{1}^\top V(\boldsymbol{\lambda}^*) + \frac{\theta}{K}V(\boldsymbol{\lambda}^*) - I, \tag{B.17}$$

where $\mathbf{1} = (1, \ldots, 1)^\top$. The matrix $V(\boldsymbol{\lambda}^*)$ in (B.17) can be evaluated as follows. At $\boldsymbol{\lambda} = \boldsymbol{\lambda}^*$, we have

$$\Delta_j = \Delta_j(\boldsymbol{\lambda}^*, \tau) = \sum_{k=1}^{K} d_{kj}\lambda_k = \frac{d}{K}.$$

Since w_j is independent of j, we may put $w_j = w$, and then (B.13) becomes

$$w = \kappa \sum_{j=1}^{K} \frac{K}{d}\, d_{ij}\left(\frac{w}{K} + 1\right) = \kappa\,(w + K)\,,$$

which yields

$$w = \frac{\kappa K}{1 - \kappa}. \tag{B.18}$$

At $\boldsymbol{\lambda} = \boldsymbol{\lambda}^*$, (B.15) becomes

$$\frac{\partial w_i}{\partial \lambda_j} = \kappa \sum_{k=1}^{K} \frac{K^2}{d^2}\, d_{ik}\left[\left(\frac{1}{K}\frac{\partial w_k}{\partial \lambda_j} + w\delta_{kj}\right)\frac{d}{K} - \left(\frac{w}{K} + 1\right)d_{jk}\right],$$

which in matrix form reads

$$W = \kappa\frac{K^2}{d^2}\, D\left[\frac{d}{K}\left(\frac{1}{K}W + wI\right) - \frac{w + K}{K}D\right]$$

with $W = (\partial w_i / \partial \lambda_j)$. With the use of (B.18), this equation can be rewritten as

$$\left(I - \kappa\frac{D}{d}\right)W = Kw\,\frac{D}{d}\left(\kappa I - \frac{D}{d}\right),$$

which is further rewritten as

$$W = Kw\left(I - \kappa\frac{D}{d}\right)^{-1} \cdot \frac{D}{d}\left(\kappa I - \frac{D}{d}\right).$$

Then the partial derivatives in (B.14) can be evaluated in matrix form as

$$V(\boldsymbol{\lambda}^*) = K\left[\kappa'\frac{D}{d} + \left(I - \kappa\frac{D}{d}\right)^{-1} \cdot \frac{D}{d}\left(\kappa I - \frac{D}{d}\right)\right]. \tag{B.19}$$

Then (B.19) shows that

$$V(\boldsymbol{\lambda}^*) \cdot \boldsymbol{\eta} = \gamma\boldsymbol{\eta} \tag{B.20}$$

with

$$\gamma = K[\kappa'\epsilon + (1 - \kappa\epsilon)^{-1} \cdot \epsilon(\kappa - \epsilon)]. \tag{B.21}$$

Multiplying (B.17) by the vector $\boldsymbol{\eta}$ in (B.4) from the right and using

$$\mathbf{1}^\top V(\boldsymbol{\lambda}^*) \cdot \boldsymbol{\eta} = \gamma\mathbf{1}^\top\boldsymbol{\eta} = 0,$$

we obtain

$$J(\boldsymbol{\lambda}^*) \cdot \boldsymbol{\eta} = \theta\left(\kappa'\epsilon + \frac{\epsilon(\kappa - \epsilon)}{1 - \kappa\epsilon} - \frac{1}{\theta}\right)\boldsymbol{\eta}.$$

Then the eigenvalue β of the Jacobian matrix $J(\boldsymbol{\lambda}^*)$ for the eigenvector $\boldsymbol{\eta}$ is expressed in terms of ϵ as

$$\beta = \Psi(\epsilon) \tag{B.22}$$

with a function Ψ defined as

$$\Psi(x) = \theta\left(\kappa' x + \frac{x(\kappa - x)}{1 - \kappa x} - \frac{1}{\theta}\right). \tag{B.23}$$

The break point τ_{break} is determined from the condition that the eigenvalue β for $\tau = \tau_{\text{break}}$ vanishes. Recall the dependence of the variables:

$$\beta \overset{\text{(B.22)}}{\longleftarrow} \epsilon \overset{\text{(B.7)}}{\longleftarrow} r \overset{\text{(B.2)}}{\longleftarrow} \tau.$$

The value ϵ^* satisfying $\Psi(\epsilon^*) = 0$ is a solution $x = \epsilon^*$ of the quadratic equation

$$\theta(bx - ax^2) - 1 = 0, \tag{B.24}$$

where

$$a = \kappa\kappa' + 1 > 0, \quad b = \kappa + \kappa' + \theta^{-1}\kappa > 0, \tag{B.25}$$

which are constants. Of the two solutions of (B.24), the larger

$$\epsilon_+^* = \frac{b + \sqrt{b^2 - 4a\theta^{-1}}}{2a} \tag{B.26}$$

is related to the first bifurcation when τ is reduced from a large value, and the smaller

$$\epsilon_-^* = \frac{b - \sqrt{b^2 - 4a\theta^{-1}}}{2a} \tag{B.27}$$

is related to the last bifurcation. We have $0 < \epsilon_-^* < \epsilon_+^*$.

By $\epsilon < 1$ in (B.8), we have $\epsilon_\pm^* < 1$, which gives the condition (29). Another (discriminant) condition $b^2 - 4a\theta^{-1} > 0$ with (B.16) and (B.25) gives (30), thereby proving Proposition 2 in Section 4.1.

The value of $r = r_\pm^{(k)}$ corresponding to $\epsilon = \epsilon_\pm^{(k)}$ is given as $r_\pm^{(k)} = \Phi^{(k)}(\epsilon_\pm^*)$ by (B.9). Then, from $r = \exp[-\tau(\sigma-1)\tilde{L}]$ in (B.2) with $\tilde{L} = 1/n = 1/6$, $\tau_\pm^{(k)}$ is given as

$$\tau_\pm^{(k)} = -\frac{6}{\sigma-1}\log r_\pm^{(k)} = -\frac{6}{\sigma-1}\log(\Phi^{(k)}(\epsilon_\pm^*)). \tag{B.28}$$

This proves (31).

Appendix B.3. Approximate formula for hexagon with $D = 3$

We search for an approximate formula of $\tau_+^{(3)}$ for the hexagon with $D = 3$ under the conditions

$$\theta \gg (\sigma/\mu)^2 \gg 1, \tag{B.29}$$

which yield

$$a \approx 1, \quad b \approx \kappa + \kappa' \approx \frac{2\mu}{\sigma-1}, \quad \epsilon_+^* \approx \frac{b}{a} \approx \frac{2\mu}{\sigma-1} \ll 1. \tag{B.30}$$

Since $\epsilon_+^* > 0$ and the numerator $\tilde{\epsilon}^{(3)}$ of (B.7) is equal to $(1-r)(1-2r)(1+r^2)$, we have

$$0 < r_+^{(3)} < \frac{1}{2}. \tag{B.31}$$

By (B.31), it is possible to introduce a fairly accurate assumption

$$(r_+^{(3)})^3 \ll 1. \tag{B.32}$$

From (B.7) for $k = 3$, we have

$$\epsilon = \frac{(1-3r+3r^2-r^3)-2r^3+2r^4}{(1+6r+12r^2+8r^3)+7r^3+2r^4} = \frac{(1-r)^3-2r^3(1-r)}{(1+2r)^3+r^3(7+2r)}.$$

Then for $r = r_+^{(3)}$ satisfying (B.32), we have

$$\epsilon_+^* \approx \left(\frac{1-r_+^{(3)}}{1+2r_+^{(3)}}\right)^3,$$

which yields

$$r_+^{(3)} = \Phi^{(3)}(\epsilon_+^*) \approx \frac{1-(\epsilon_+^*)^{1/3}}{1+2(\epsilon_+^*)^{1/3}}.$$

Then from (B.28) with (B.30), we obtain

$$\begin{aligned} \tau_+^{(3)} &\approx -\frac{n}{\hat{L}(\sigma-1)}\log\left(\frac{1-(\epsilon_+^*)^{1/3}}{1+2(\epsilon_+^*)^{1/3}}\right) \\ &\approx 18\cdot 2^{1/3}\frac{\mu^{1/3}}{(\sigma-1)^{4/3}}, \end{aligned} \tag{B.33}$$

Table B.1: Relative error of the approximation (B.33) for $\tau_+^{(3)}$.

$r_+^{(3)}$	0.0	0.1	0.2	0.3	0.4	0.5
True value of $\tau_+^{(3)}$ ($\sigma = 5.0$)	0.00	0.687	0.726	0.704	0.664	0.620
Approximate value of $\tau_+^{(3)}$ ($\sigma = 5.0$)	0.00	0.692	0.748	0.749	0.733	0.710
Error (%)	0.0	0.75	3.01	6.40	10.4	14.4

which proves Proposition 4 in Section 4.1. This formula (B.33) is fairly accurate as shown in Table B.1, which lists the relative error of the $\tau_+^{(3)}$:

$$\text{Error} = |[(\text{Approximate value}) - (\text{Exact value})]/(\text{Exact value})| \times 100 \quad (\%).$$

Appendix B.4. Order of emerging hexagons

When r (or τ) is changed continuously, the first and the last bifurcations engendering hexagons are most important bifurcations. It is possible to predetermine the order of the emergence of such hexagons as expounded below.

To begin with, under the condition (B.8), the flat earth equilibrium is stable for a large τ $(= +\infty)$ because $\tau = +\infty$ entails $\epsilon = 1$ via (B.2) and (B.7) and then the eigenvalue β in (B.22) with (B.23) becomes negative under the condition (29).

The functions $\epsilon(r) = \tilde{\epsilon}^{(k)}(r)/d$ for $k = 3, 4, 9, 12, 36(\mathrm{I}), 36(\mathrm{II})$ in the range $0 < r < 1$ are plotted in Fig. B.1. Then, for a $\epsilon = \epsilon_\pm^*$, the associated $r = r_\pm^{(k)} = \Phi^{(k)}(\epsilon_\pm^*)$ of (B.9) satisfies inequalities

$$r_+^{(3)} < r_+^{(k)} < r_+^{(36(\mathrm{I}))}, \quad r_-^{(3)} < r_-^{(k)} < r_-^{(36(\mathrm{I}))}, \quad k = 4, 9, 12, 36(\mathrm{II}).$$

Then from (B.2), for the associated transport cost parameter $\tau_\pm^{(k)}$, we have

$$\tau_+^{(3)} > \tau_+^{(k)} > \tau_+^{(36(\mathrm{I}))}, \quad \tau_-^{(3)} > \tau_-^{(k)} > \tau_-^{(36(\mathrm{I}))}, \quad k = 4, 9, 12, 36(\mathrm{II}).$$

Hence, when τ is reduced from a large value, the first bifurcation is associated with $\tau_+^{(3)}$ $(> \tau_-^{(3)})$ for $D = 3$ and the last one to $\tau_-^{(36(\mathrm{I}))}$ $(< \tau_+^{(36(\mathrm{I}))})$ for $D = 36(\mathrm{I})$. This proves Proposition 5 in Section 4.2.

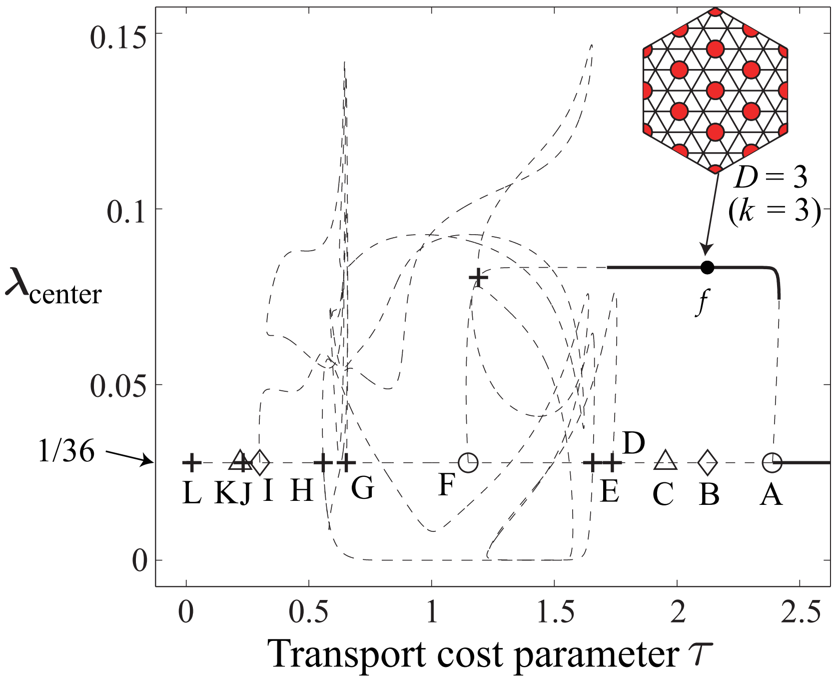

Figure C.1: Equilibrium curves related to Lösch's hexagons other than those given in Fig. 10. Solid curves represent stable equilibria and dashed ones represent unstable ones.

Appendix C. Bifurcating equilibria on a hexagonal lattice without boundary

For the 6×6 hexagonal lattice, the equilibrium curves for stable Lösch's hexagons are given in Fig. 10, while other equilibrium curves are given in this appendix.

- Equilibria for hexagons other than those given in Fig. 10 are shown in Fig. C.1.
- The equilibrium curves for racetracks and associated agglomeration patterns are shown in Fig. C.2.
- The semi-square pattern (point n) and the two places (point l) are shown in Fig. C.3.
- Several long narrow patterns have been found to branch from the flat earth equilibria, as shown in Fig. C.4, which are all unstable except for the discrete long narrow pattern at point m.

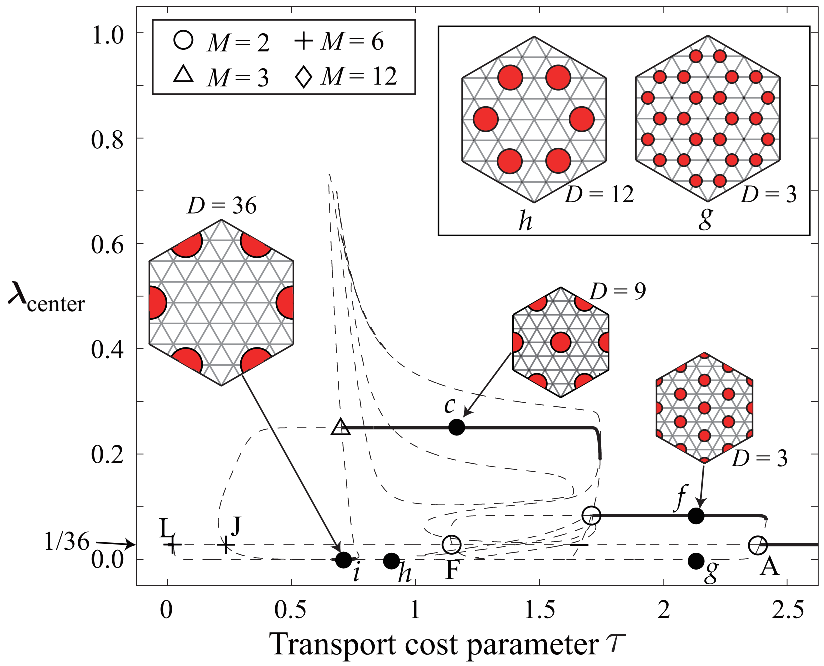

(a)

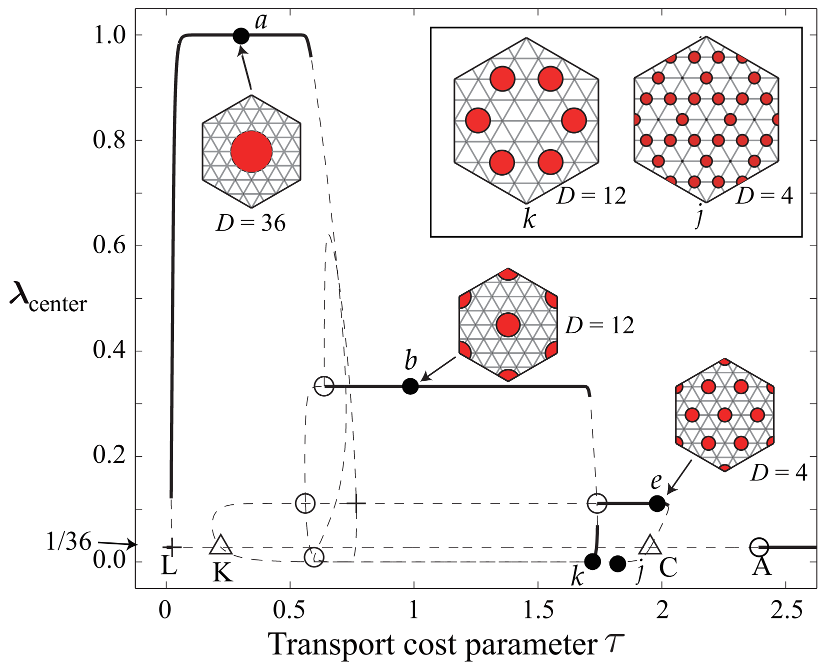

(b)

Figure C.2: Equilibrium curves related to racetracks and associated population distributions displayed in the hexagonal windows. Solid curves represent stable equilibria and dashed ones represent unstable ones.

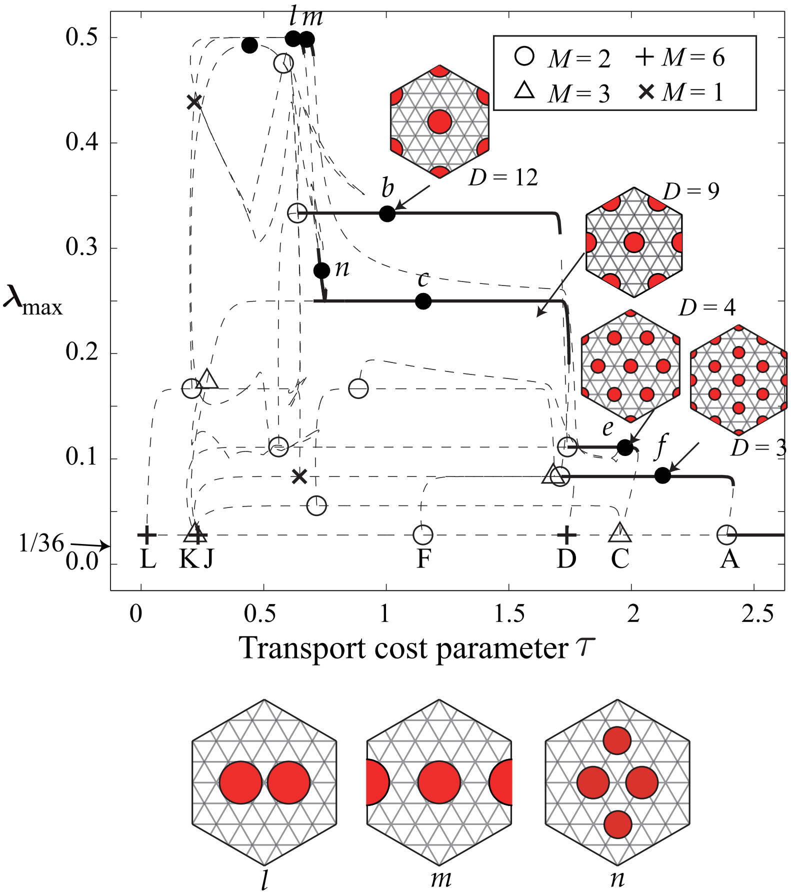

Figure C.3: Equilibrium curves related to two places and semi-square pattern and associated population distributions displayed in the hexagonal windows. The ordinate λ_{max} means the maximum population among 36 places on the hexagonal lattice, solid curves represent stable equilibria, and dashed ones represent unstable ones.

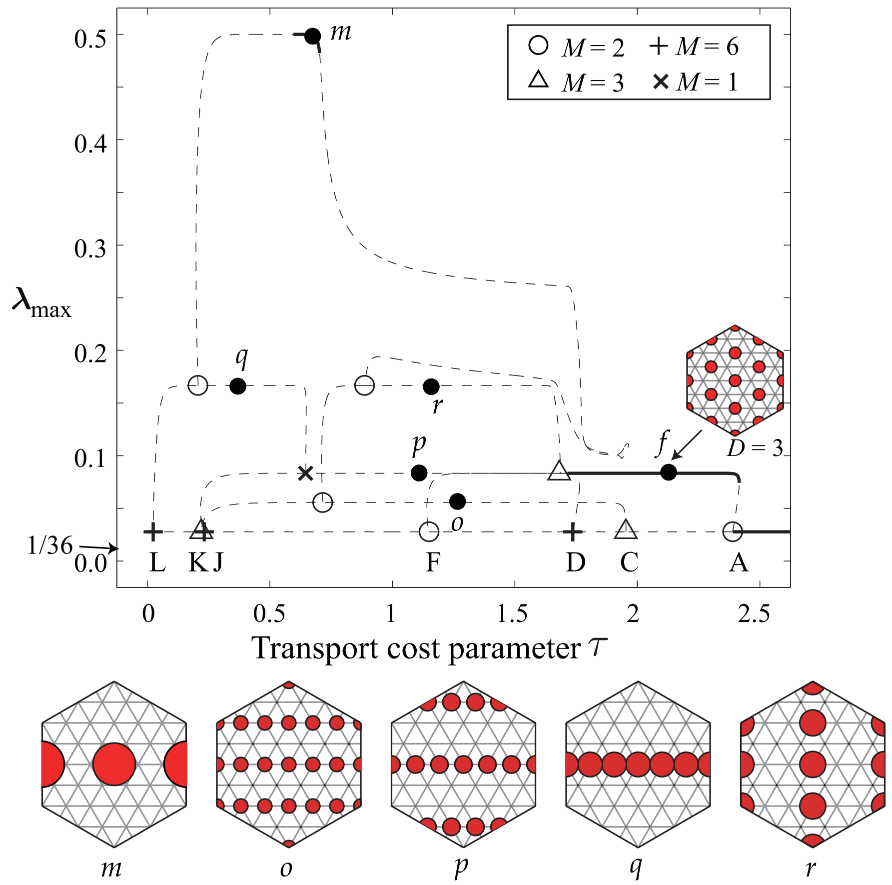

Figure C.4: Equilibrium curves related to long narrow patterns and associated population distributions displayed in the hexagonal windows. Solid curves represent stable equilibria and dashed ones represent unstable ones.

Appendix D. Agglomeration behaviors of the hexagonal lattice with boundary

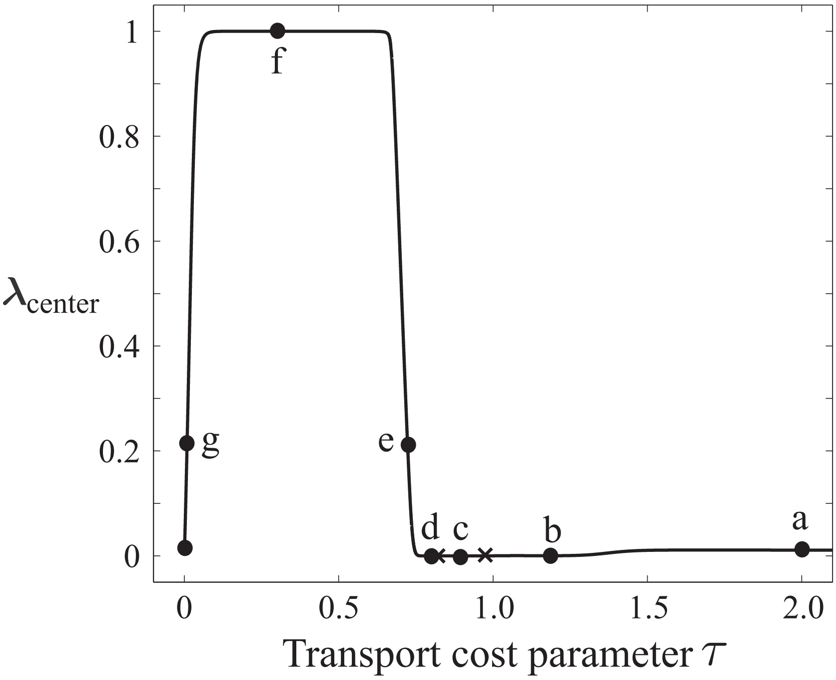

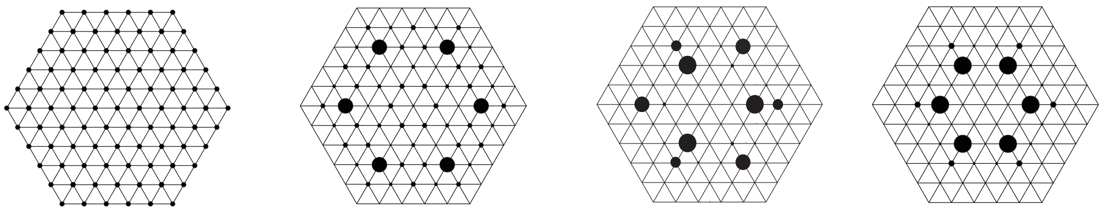

point a (τ = 2.000) (Flat earth) | point b (τ = 1.200) | point c (τ = 0.900) (Triangle) | point d (τ = 0.809) (Racetrack)

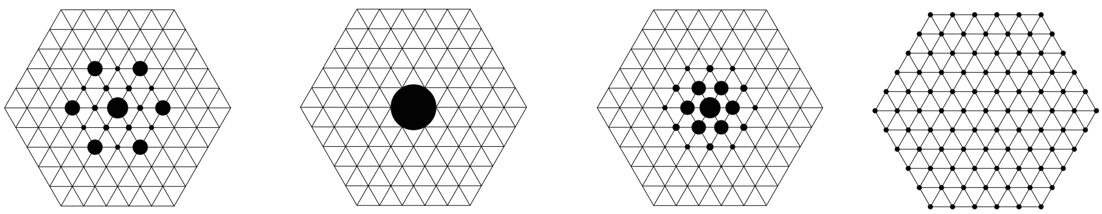

point e (τ = 0.717) | point f (τ = 0.300) (Atomic mono-center) | point g (τ = 0.012) (Megalopolis) | point h (τ = 0.000) (Flat earth)

Figure D.1: Equilibrium curves and associated population distributions for $(\sigma, \mu) = (5.0, 0.1)$. ($\times$) denotes a simple bifurcation point and a bifurcated curve between two simple bifurcation points is stable.

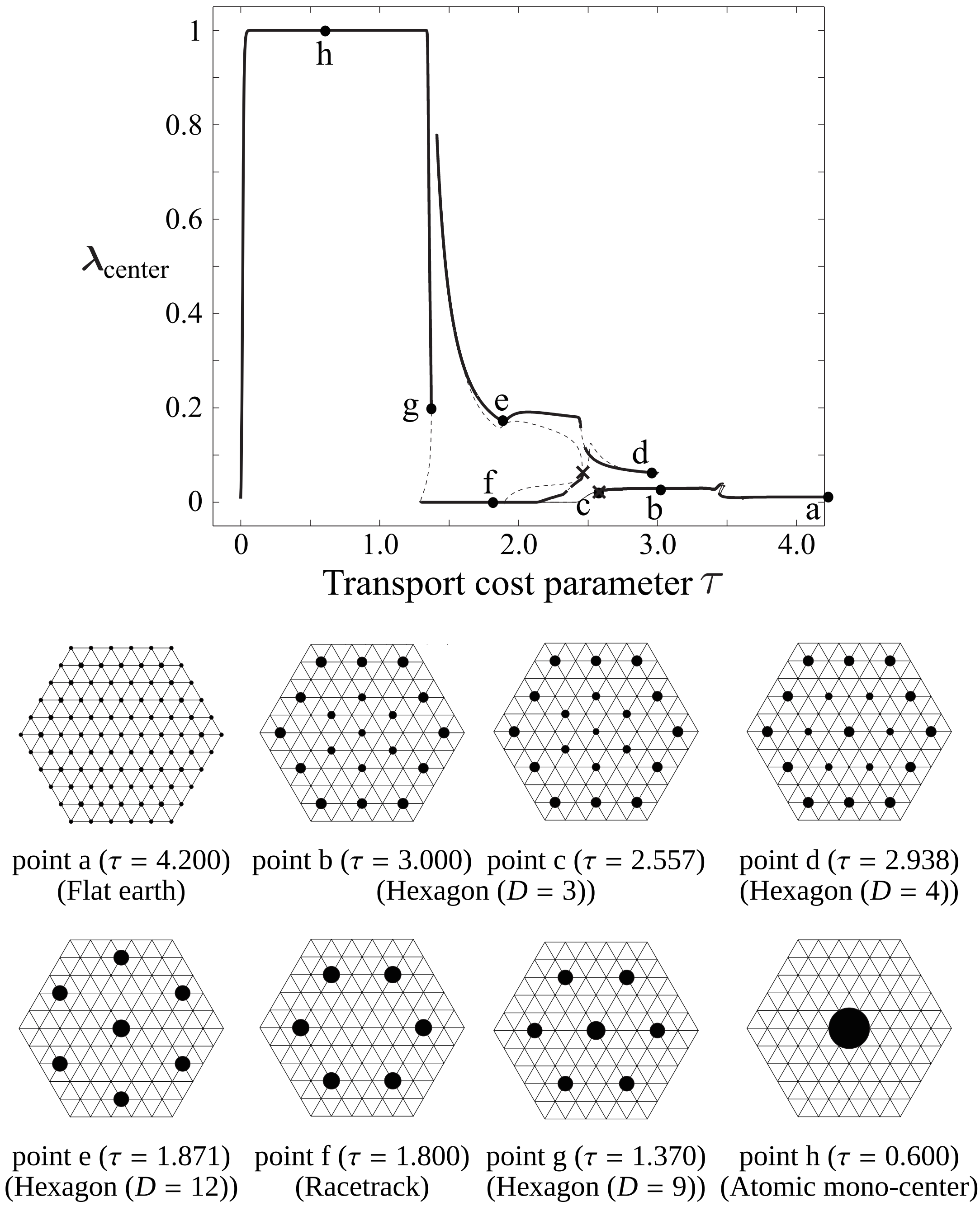

Figure D.2: Equilibrium curves and associated population distributions for $(\sigma, \mu) = (4.0, 0.4)$. ($\times$) denotes a simple bifurcation point.

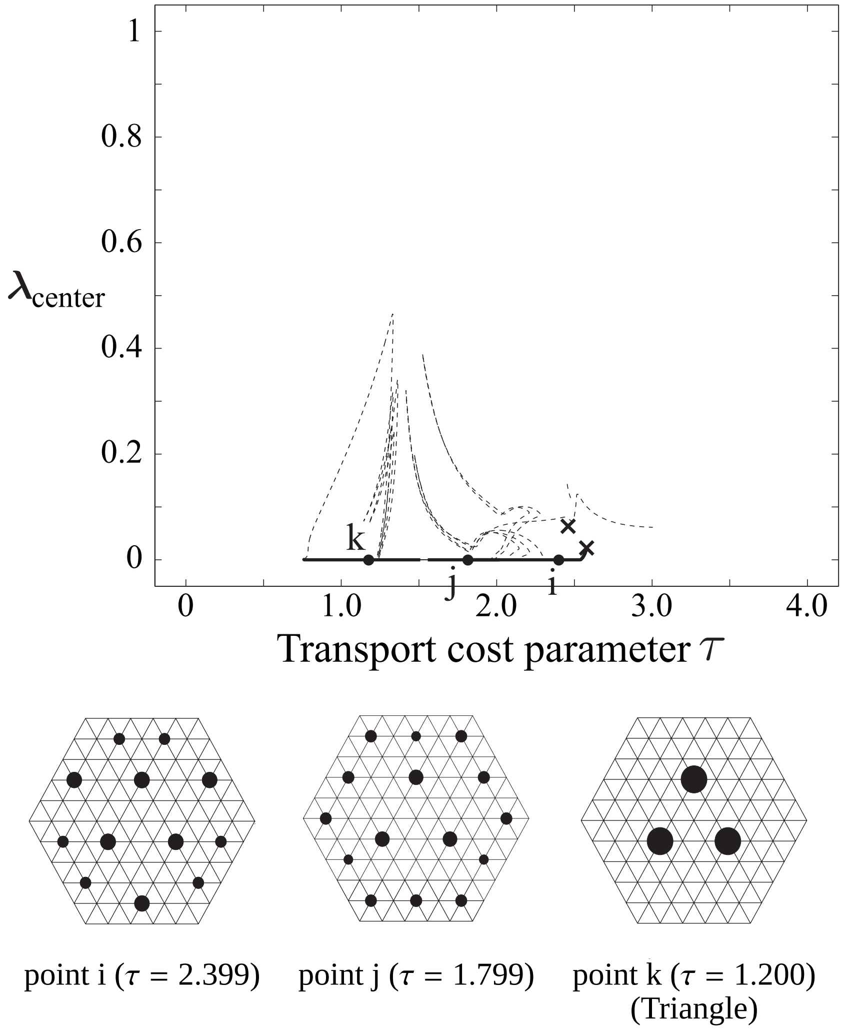

Figure D.3: Bifurcated equilibrium curves and associated population distributions for $(\sigma, \mu) = (4.0, 0.4)$. ($\times$) denotes a simple bifurcation point.

A case with $(\sigma, \mu) = (5.0, 0.1)$ has a weaker agglomeration force in comparison with the standard case with $(\sigma, \mu) = (5.0, 0.4)$. As shown by the equilibrium curves and associated population distributions in Fig. D.1, no hexagonal agglomerations are observed.

Another case with $(\sigma, \mu) = (4.0, 0.4)$ has a stronger agglomeration force in comparison with the standard case with $(\sigma, \mu) = (5.0, 0.4)$. Figure D.2 shows equilibrium curves with two bifurcation points ($\times$) and Fig. D.3 shows equilibrium curves branching from these bifurcation points. These curves are looping and multiple stable equilibria are present due to the increase of agglomeration force. The hexagons with $D = 3$ and $D = 4$ coexist as stable equilibria during $2.59 < \tau < 2.97$.